Title

Cytotoxic CD4+ tissue-resident memory T cells are associated with asthma severity.

Journal

Med, 4(12)

Authors

Herrera-De La Mata, Sara
Ramírez-Suástegui, Ciro
Mistry, Heena
et al.

Publication Date

2023-12-08

DOI

10.1016/j.medj.2023.09.003

Peer reviewed

HHS Public Access
Author manuscript
Med. Author manuscript; available in PMC 2024 December 08.

Published in final edited form as:
Med. 2023 December 08; 4(12): 875–897.e8. doi:10.1016/j.medj.2023.09.003.

Cytotoxic CD4+ tissue-resident memory T cells are associated with asthma severity

Sara Herrera-De La Mata[1,8], **Ciro Ramírez-Suástegui**[1,8], **Heena Mistry**[1,2,3,4,8], **Francisco Emmanuel Castañeda-Castro**[1], **Mohammad A. Kyyaly**[2,4], **Hayley Simon**[1], **Shu Liang**[1], **Laurie Lau**[2,3], **Clair Barber**[3], **Monalisa Mondal**[1], **Hongmei Zhang**[5], **Syed Hasan Arshad**[2,3,4], **Ramesh J Kurukulaaratchy**[2,3,4,9,*], **Pandurangan Vijayanand**[1,6,7,9,*], **Grégory Seumois**[1,9,10,*]

[1]La Jolla Institute for Immunology, La Jolla, CA 92037, United States.

[2]Clinical and Experimental Sciences, Faculty of Medicine, University of Southampton, Southampton SO16 6YD, United Kingdom.

[3]National Institute for Health Research Southampton Biomedical Research Centre, University Hospital Southampton Foundation Trust, Southampton SO16 6YD, United Kingdom.

[4]The David Hide Asthma and Allergy Research Centre, St Mary's Hospital, Newport, Isle of Wight PO30 5TG, United Kingdom.

[5]Division of Epidemiology, Biostatistics, and Environmental Health, School of Public Health, University of Memphis, Memphis, TN 38152, United States.

[6]Department of Medicine, University of California San Diego, La Jolla, CA 92037, United States.

[7]Institute of Systems, Molecular and Integrative Biology, University of Liverpool, Liverpool L69 3BX, United Kingdom.

[8]These authors contributed equally

[9]Senior author

[10]Lead contact

[*]Correspondence: Ramesh J Kurukulaaratchy (r.j.kurukulaaratchy@soton.ac.uk); Pandurangan Vijayanand (vijay@lji.org); Grégory Seumois (gregory@lji.org).

AUTHOR CONTRIBUTIONS

Conceptualization, R.J.K, S.H.A., P.V., and G.S.; project lead, S.H-M., C.R-S., H.M., R.J.K., S.H.A., P.V., and G.S.; methodology, sample and clinical data collection, H.M., M.A.K., L.L., C.B., R.J.K., S.H.A., and G.S.; resources, H.M., R.J.K., S.H.A., P.V., and G.S.; performed experiments, S.H-M., H.M., and G.S.; performed sequencing library preparation and sequencing runs, S.H-M., H.S., S.L., and M.M.; performed computational and bioinformatic analysis, C.R-S. and F.E.C-C.; performed statistical analysis, S.H-M., C.R-S., and H.Z.; unrestricted access to data, S.H-M., C.R-S., H.M., F.E.C-C., S.H.A., R.J.K., P.V., and G.S.; data analysis and interpretation, S.H-M., C.R-S., H.M., F.E.C-C., P.V., and G.S.; writing and editing manuscript, S.H-M., C.R-S., H.M., P.V., and G.S.; review of manuscript, all authors; funding and supervision, R.J.K., S.H.A., P.V., and G.S. All authors read and approved the final article and take responsibility for its content.

DECLARATION OF INTERESTS

All authors declare that they have no relevant conflicts of interest. S.H.A received research funding unrelated to this work from Dyson Inc.

SUMMARY

Background—Patients with severe uncontrolled asthma represent a distinct endotype with persistent airway inflammation and remodeling that is refractory to corticosteroid treatment. $CD4^+$ T_H2 cells play a central role in orchestrating asthma pathogenesis, and biologic therapies targeting their cytokine pathways have had promising outcomes. However, not all patients respond well to such treatment, and their effects are not always durable nor reverse airway remodeling. This observation raises the possibility that other $CD4^+$ T cell subsets and their effector molecules may drive airway inflammation and remodeling.

Methods—We performed single-cell transcriptome analysis of >50,000 airway $CD4^+$ T cells isolated from bronchoalveolar lavage (BAL) samples from 30 patients with mild and severe asthma.

Findings—We observed striking heterogeneity in the nature of $CD4^+$ T cells present in asthmatics' airways with tissue-resident memory (T_{RM}) cells making a dominant contribution. Notably, in severe asthmatics, a subset of $CD4^+$ T_{RM} cells (CD103-expressing) was significantly increased, comprising nearly 65% of all $CD4^+$ T cells in the airways of male patients with severe asthma when compared to mild asthma (13%). This subset was enriched for transcripts linked to T cell receptor (TCR) activation (*HLA-DRB1, HLA-DPA1*) and cytotoxicity (*GZMB*, *GZMA*) and, following stimulation, expressed high levels of transcripts encoding for pro-inflammatory non-T_H2 cytokines (CCL3, CCL4, CCL5, TNF, LIGHT) that could fuel persistent airway inflammation and remodeling.

Conclusions—Our findings indicate the need to look beyond the traditional T2 model of severe asthma to better understand the heterogeneity of this disease.

eTOC blurb:

Using single-cell transcriptomics, Herrera-De La Mata *et al*. report that CD103-expressing $CD4^+$ T_{RM} cells with cytotoxic and pro-inflammatory features are increased in the airways of males with severe asthma and are likely to contribute to the pathogenesis of asthma severity.

Graphical Abstract

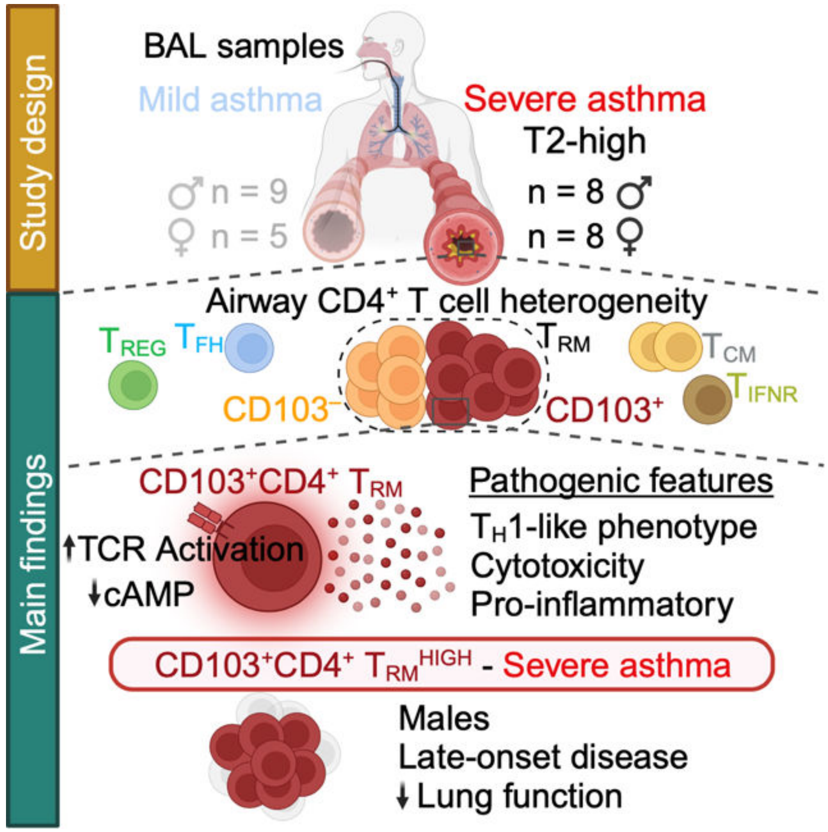

INTRODUCTION

Asthma is one of the most common chronic diseases affecting children and adults.[1–4] The classical symptoms of asthma like wheeze, cough, and breathlessness, are triggered by inflammation and remodeling of the airways that results in airway hyperreactivity and obstruction.[2,5,6] The airway inflammation in asthmatic patients is considered to be driven by type 2 cytokine-producing CD4$^+$ T cells (T$_H$2) that play a central role in orchestrating recruitment and activation of innate immune cells such as eosinophils, basophils, and mast cells.[2,3,5–7] Suppressing airway inflammation with corticosteroids remains the mainstay of treatment for most patients with asthma.[8–10] However, many patients with severe forms of asthma fail to respond well to corticosteroids and suffer from persistent symptoms and recurrent life-threatening exacerbations.[8] Moreover, the recently approved biological agents blocking type 2 cytokines or immunoglobulin (Ig) E are neither uniformly effective nor do they reverse disease pathogenesis in severe asthmatics.[3,11–14] These observations raise the possibility that other effector CD4$^+$ T cells may contribute to airway inflammation and remodeling in severe asthmatics.

Functional studies in model organisms have implicated a wide-range of CD4$^+$ T cell subsets such as T$_H$2, T$_H$9, T$_H$17, T$_H$1, follicular helper T (T$_{FH}$) cells, and tissue-resident memory T (T$_{RM}$) cells in the pathogenesis of allergic airway inflammation.[2,15–23] In murine models, T$_{RM}$ cells have also been shown to have features that could support airway remodelling and fibrosis, important facets of severe asthma.[2,24–26] Because T$_{RM}$ cells are mainly localized to the barrier sites[27] with only a very minor population recirculating in the blood, understanding the biology of T_{RM} cells in asthma would require analysis of airway specimens.[26,28,29] Targeted immunophenotyping studies performed in airway specimens from asthmatic patients have shown associations for certain $CD4^+$ T cell subsets with asthma pathogenesis.[21,29–31] However, these studies do not provide an unbiased and precise characterization of $CD4^+$ T cell subsets associated with asthma severity. The difficulty in obtaining airway specimens from severe asthmatics and limitations in the number of cells available for research have further compounded this problem. Single-cell genomic assays offer an attractive solution to address this problem in a hypothesis-free manner, and, importantly, such studies have yielded vital insights into the pathogenesis of human autoimmune diseases and cancer.[32–39] While a recent single-cell transcriptomic study reported significant increase in the proportion of T_H2 cells in patients with mild asthma compared to healthy controls,[40] it is not known whether this observation holds true for severe disease or if other $CD4^+$ T cell subsets are involved as well.

Here, to define the $CD4^+$ T cell subsets and their properties associated with severe asthma and corticosteroid resistance, we performed single-cell RNA-seq assays from purified $CD4^+$ T cells isolated from the airways of patients with severe and mild asthma. Our unbiased approach found a significant association between the abundance of cytotoxic $CD4^+$ T_{RM} cells and asthma severity in males that we hypothesize is uniquely relevant for driving their airway inflammation and remodeling.

RESULTS

Single-cell transcriptomic analysis reveals heterogeneity among airway $CD4^+$ T cells in asthma

To understand why the disease phenotype shifts from an easily treatable and largely reversible condition in mild asthma to a permanent airway inflammation and impaired lung function in severe asthma, we focused our analysis to specifically identify differences in the properties of $CD4^+$ T cells present in the airways of severe asthmatic patients. We performed bronchoscopy and collected bronchoalveolar lavage (BAL) from patients with severe asthma (n=16, 50% male) from the Wessex AsThma CoHort of difficult asthma (WATCH) study,[41] which has extensively characterized patients with severe asthma requiring ‘high dose’ and/or ‘continuous or frequent use of oral corticosteroid’, in accordance with global initiative of asthma (GINA) management step 4 and 5[42,43] (Figure 1A; and Table S1A). To specifically identify differences that are associated with asthma severity, as controls, we enrolled patients with mild asthma (n=14, 64% male) (Figure 1A; and Table S1A). At the time of bronchoscopy, the majority of mild asthmatic patients (10/14) were on inhaled steroids, but at a significantly lower dose than the severe asthmatic patients, as it would be unethical to withhold them from regular asthma medications (Table S1A). By only using non-asthmatic patients as controls, we would have failed to discriminate changes that are linked to asthma *versus* asthma severity. However, we have included data from published studies[29,44–49] to draw relevant comparisons with non-asthmatic subjects.

To define the airway $CD4^+$ T cell subsets specifically associated with asthma disease severity and potentially contributing to persistent inflammation and unresponsiveness to current asthma treatment, we isolated and purified $CD4^+$ T cells (n >40,000) from BAL specimens and performed single-cell RNA-seq assay using the oil droplet-based platform (10x Genomics). After exclusion of doublets and low-quality transcriptomes, clustering analysis of airway $CD4^+$ T cells (n=27,771 cells; median ~1,304 cells/donor) revealed 8 transcriptionally distinct subsets (see STAR Methods; Figure 1B; Figures S1A-D; and Tables S2A-C).

The molecular identity for each cluster was determined based on enrichment analysis of canonical markers and signature gene lists linked to established $CD4^+$ T cell subsets (Figures 1C and 1D; Figures S1E and S1F; and Tables S2C and S3A). The two largest clusters (cluster 1 and 2), representing 71% of all $CD4^+$ T cells analyzed, were significantly enriched for T_{RM} signature genes[40,50,51] (Figures 1D-F; and Figure S1E), and thus were defined as T_{RM} cells. Notably, both T_{RM} clusters expressed high levels of the T_{RM} marker gene *CD69*[51] (Figure 1D), whereas T_{RM} cells in cluster 1 expressed higher levels of another T_{RM} marker gene, *ITGAE* (Figure 1D and 1G), which encodes for the alpha chain of the integrin CD103, a transmembrane protein required for the adhesion of T cells to E-cadherin expressed by epithelial cells.[50,52,53] By labeling BAL cells with anti-CD69 and anti-CD103 DNA-barcoded antibodies prior to performing single-cell RNA-sequencing, we confirmed the enrichment of CD103-expressing T_{RM} cells in cluster 1 (Figure 1H); henceforth, for simplicity, we refer to cluster 1 and 2 as $CD103^+$ T_{RM} and $CD103^-$ T_{RM} clusters, respectively.

The third largest cluster (cluster 3=13% of airway $CD4^+$ T cells) was enriched for the expression of gene signatures linked to central memory T (T_{CM}) cells[50,54–56] (Figure 1D; and Figure S1E). Cluster 4 (4%) and 5 (4%) cells were enriched for gene signatures linked to regulatory T cells (T_{REG})[57,58] and T_{FH} cells,[59] respectively (Figure 1D; and Figure S1E). Cluster 6 (3%) was highly enriched for type I and II interferon response gene signatures reminiscent of the recently described interferon response genes expressing helper T cell subset (T_{IFNR}) with a potential regulatory function in allergy[22] (Figure 1D; and Figure S1E). Two other relatively small clusters of cells, cluster 7 (1%), enriched for cell cycle signature genes, represented proliferating cells,[60] and cluster 8 (1%), which expressed high levels of several transcripts encoding for cytotoxicity molecules (GNLY, PRF1, GZMB), represented cytotoxic $CD4^+$ T cells[61] (Figure 1D; and Figure S1E). Gene set enrichment analysis for signatures linked to canonical T helper (T_H) effector subsets (Figure S1E; and Table S3A) showed significant positive enrichment of T_H1 signature genes in $CD103^+$ T_{RM} cluster, but T_H17 and T_H2 signature genes were not positively enriched in any of the $CD4^+$ T cell clusters (Figures S1E and S1G). Overall, our results highlight a substantial level of heterogeneity in the profile of $CD4^+$ T cells present in the asthmatic airways, with T_{RM} subsets making up a major contribution.

$CD103^+$ T_{RM} cells are significantly increased in the airways of males with severe asthma

We next determined the $CD4^+$ T cell subsets that were quantitatively increased in the airways of patients with severe asthma and assessed their association with clinical and physiological parameters of asthma severity. Because biological sex has been shown to stratify severe asthmatics into distinct endotypes, where males with severe asthma display

Author Manuscript
Author Manuscript
Author Manuscript

poor lung function and high use of maintenance corticosteroids,[62,63] we also explored the influence of biological sex on the composition of airway CD4$^+$ T cells in severe asthma. Among the CD4$^+$ T cell subsets, the proportion of cells in the CD103$^+$ T$_{RM}$ subset was significantly increased in the airways of patients with severe asthma compared to mild asthma (46% *versus* 21%; $P < 0.05$), while the proportions of CD103$^-$ T$_{RM}$ subset were significantly decreased (22% *versus* 44%; $P < 0.05$) (Figure S2A). Interestingly, while the proportions of the CD103$^+$ T$_{RM}$ subset were not significantly different between males and females (Figure S2B), we observed that the increase in the proportion of CD103$^+$ T$_{RM}$ subset was significant only when comparing male patients with severe and mild asthma (Figures 2A-C; 64% *versus* 13% of all CD4$^+$ T cells in severe *versus* mild asthma; $P < 0.01$). The proportions of the CD103$^-$ T$_{RM}$ cluster as well as the T$_{CM}$ cluster were significantly lower in male severe asthmatics (Figures 2A-C; $P < 0.01$ and $P < 0.05$, respectively). All other airway CD4$^+$ T cell subsets showed no significant differences between mild and severe asthmatics in both males and females (Figure 2C; and Figure S2C).

We validated the findings from single-cell transcriptome analysis by performing flow cytometric analysis of BAL cells from the same study participants. Based on the expression of cell surface markers, we classified airway CD4$^+$ T cells into 5 subsets: two types of T$_{RM}$ cells (CD69$^+$CD103$^-$, CD69$^+$CD103$^+$), non-T$_{RM}$ cells (CD69$^-$), follicular helper T cells (T$_{FH}$, CXCR5$^+$GITR$^-$), and regulatory T cells (T$_{REG}$, CXCR5$^-$CD127$^+$CD25$^+$) (Figures 2D and 2E; Figures S2D-G; and Table S1D). As expected, we found that the proportions of CD103$^+$ T$_{RM}$ cells were significantly increased in males with severe asthma (50%) compared to mild asthma (22%) (Figure 2D; $P < 0.001$). We observed no significant differences in the proportions of CD103$^+$ T$_{RM}$ cells between males with severe asthma who are currently on or off maintenance oral corticosteroids [OCS] or biologics (Figure 2F; and Tables S1A and S2A). Together, these findings establish a significative association between the frequency of CD103$^+$ T$_{RM}$ cells and asthma severity in male asthmatic patients that is not dependent on drug treatments.

We then performed unbiased Spearman correlation analysis in a sex-specific manner to investigate any association between the identified CD4$^+$ T cell clusters with clinical and physiological parameters related to asthma severity (Figure S2H; and Table S1A and S1E). Among the significant associations (Figure S2H), we observed a positive correlation between the proportions of CD103$^+$ T$_{RM}$ cell subset and a composite asthma severity score (adapted from the Asthma Severity Scoring System [ASSESS])[64] in male but not female asthmatics ($r_S = 0.8$ and $P < 0.01$; Figure 2G; Figure S2H; and Table S1E). The composite asthma severity score is a score ranging from 0–20 from the Severe Asthma Research Program [SARP][65] comprising of measurement of asthma symptoms, quality of life, degree of airflow obstruction, use of corticosteroids or biologics, and frequency of asthma exacerbations requiring oral corticosteroids and hospitalization (Figure 2G; Figure S2H; and Tables S1A and S1B). This asthma severity score was used at the time of bronchoscopy to classify these asthmatic patients (not at the time of diagnosis), and its reliability has been recently validated,[66] providing a more objective measure of the magnitude of treatment response in individual patients and phenotypic groups.[64] We also found a significant positive correlation with the severity of airflow obstruction (using post-bronchodilator FEV$_1$ and FEV$_1$/FVC) in males ($r_S = 0.7$ and $P < 0.01$; Figure 2G; Figure S2H; and Tables S1A and S1E). Notably, the proportions of airway T_{REG} cells were negatively correlated with the proportions of $CD103^+$ T_{RM} cell subset in males ($r_S = 0.7$ and $P < 0.05$) and with the severity of airflow obstruction in males (Figures S2H and S2I; and Table S1E), suggesting a potential imbalance between $CD103^+$ T_{RM} and T_{REG} subsets in the airways of males with severe asthma. Finally, we found that age was positively correlated with the proportions of $CD103^+$ T_{RM} subset in the airways of male severe asthmatics ($r_S = 0.7$ and $P < 0.05$; Figures S2H and S2J; and Table S1E). The fact that 7 of the 8 male participants studied developed late-onset severe asthma (age >40 years), suggests that older age and late-onset of disease may also be linked to this specific immune profile observed in males with severe asthma (Figures S2H and S2J). To specifically address if older age as opposed to the male severe asthma phenotype was associated with increased frequency of $CD103^+$ T_{RM} cells in the airways, we re-analyzed three published BAL T cell datasets from non-asthmatic healthy subjects (Table S1F)[29,44,45]. We observed that the proportion of $CD103^+$ T_{RM} cells in BAL samples from non-asthmatic healthy subjects was lesser (mean = 16%) when compared to our data in males with severe asthma (mean = 50%) (Figures 2D and 2H; and Table S1F). Notably, in the study by Tang *et al.*, 2022 (#2),[45] 18 of the 20 study participants were older than 60 years (Table S1F), suggesting that older age *per se* is not associated with increased frequency of $CD103^+$ T_{RM} cells in the airways. Furthermore, our re-analysis of BAL data from the recent study by Camiolo *et al.*, 2021 (#3),[29] which also included patients with mild and severe asthma, showed high frequency of $CD103^+$ T_{RM} cells only in some patients in the severe asthma group but not those in the mild asthma or healthy control groups, thus strengthening the association with asthma severity (Figure 2H; and Table S1F).

$CD103^+$ T_{RM} subset displays qualitative features linked to TCR activation and cytotoxicity

To determine the molecular properties of cells in the $CD103^+$ T_{RM} subset that may contribute to the pathogenesis of asthma severity, we first compared expression profiles of cells from the $CD103^+$ T_{RM} subset (cluster 1) with those from the $CD103^-$ T_{RM} subset (cluster 2) across all patient groups, using sex as a covariate. We observed major transcriptional differences between the two T_{RM} subsets with over 1,300 differentially expressed transcripts (Figure 3A; and Table S2D), and, importantly, these differences were mostly preserved when differential gene expression analysis (DGEA) between the two T_{RM} subsets was performed separately in males and females (Figure 3B; and Table S2E). Several genes involved in cytotoxic function (*GZMB*, *GZMA*, *GZMH*, *FASLG*)[61] were increased in expression in the $CD103^+$ T_{RM} subset (Figures 3A and 3B; and Table S2D and S2E). In addition, to evaluate the effect of treatment, we compared the expression profiles between both T_{RM} cell subsets across all patient groups using treatment (both OCS and biologics) as a covariate (Figure S3A; and Table S2F). We observed a positive correlation ($R = 1$, $P < 0.0001$) when comparing the results of DGEA between both T_{RM} subsets using sex or treatment as a covariate, with the vast majority of the genes being shared by both analyses (Figures S3B and S3C; and Table S2G), suggesting treatment is not a major confounding factor.

Unbiased ingenuity pathway analysis (IPA) of transcripts with increased expression in the $CD103^+$ T_{RM} subset showed significant enrichment for multiple T-cell associated biological pathways (Figure 3C; and Table S3B). The most enriched pathway was the

T_H1 pathway (*CXCR3*, *IFNG*), confirming that the CD103$^+$ T_{RM} subset is enriched for T_H1 features. Secondly, the integrin signaling pathway (*ITGAE*, *ITGA1*, *ITGB2*), which plays an important role in mediating interactions of CD103$^+$ T_{RM} subset with epithelial cells and extracellular matrix. Finally, we observed significant enrichment of genes involved in T cell receptor (TCR) signaling, CD28 and ICOS co-stimulation pathways (*NFATC2*, *CSK*, *LAT*, *LCP2*, *CD40LG*, *CD52*, *HLA-DRB1*, *HLA-DRB5*, *HLA-DRA, MIR155HG*), and survival pathways (ERK/MAPK signaling), and confirmed this finding by gene set enrichment analysis (GSEA) and gene set variation analysis (GSVA) ($P < 0.001$) (Figures 3C-F; Figure S3D; and Tables S2H, S3A, and S3B). Notably, HLA-DR expression has been reported to mark recently activated T cells following *in vivo* antigen-specific TCR engagement[67,68], suggesting that the CD103$^+$ T_{RM} subset may be enriched for T cells that were recently activated in the asthmatic airways (Figure 3D). Furthermore, transcripts encoding for several cytokines (IFN-γ, TNF, LIGHT/TNFSF14) and chemokines (CCL4/MIP-1β, CCL5/RANTES), known to be involved in promoting airway inflammation and remodeling,[69–71] showed significant increased expression in the CD103$^+$ T_{RM} subset (Figure 3D). Notably, despite treatment with high-dose corticosteroid and/or biological agents, the sustained expression of transcripts linked to TCR activation and cytokines in the CD103$^+$ T_{RM} subset (Figure 3D) suggests that treatment fails to curtail the activation and functional responses of airway CD103$^+$ T_{RM} cells in severe asthma.

GSEA analysis as well as single-sample GSVA ($P < 0.0001$) showed significant positive enrichment of cytotoxicity signature genes in the CD103$^+$ T_{RM} subset (*GZMB*, *GZMA*, *GZMH*, *FASLG*)[61] (Figures 3A, 3C, 3G-I; Figure S3D; and Tables S2D and S2H), indicating that cytotoxic CD4$^+$ T cells were enriched in the CD103$^+$ T_{RM} subset. In addition, treatment with either OCS or biologics in severe asthmatics was associated with increased expression of *CCL4* and *GZMH* transcripts in the CD103$^+$ T_{RM} cluster (Figures S3E and S3F; and Tables S2I and S2J). The CD103$^+$ T_{RM} subset also showed increased expression of transcripts encoding for two transcription factors linked to cytotoxic function in T cells: HOBIT (*ZNF683*), which is linked to T_{RM} differentiation and persistence of cytotoxic effector T cells,[50,72,73] and *HOPX*, known to regulate *GZMB* expression[74] and to increase *in vivo* persistence of T_H1 cells, by reducing sensitivity to FAS-mediated apoptosis of T cells[75,76] (Figure 3G). Together, these findings suggest that the CD103$^+$ T_{RM} subset is enriched for cells with increased cytotoxicity and effector properties, potentially driving airway inflammation and remodeling in severe asthma. Of note, bulk transcriptomic analysis of sorted CD103$^+$ T_{RM} cells confirmed the increased expression of transcripts encoding for cytotoxicity-associated molecules like Granzyme B and the transcription factor HOBIT ($P < 0.0001$) (Figures S3G and S3H; and Table S4A). Using *GZMB* gene expression as a phenotypic marker for cytotoxic CD4$^+$ T cells, we confirmed that the frequency of *GZMB*-expressing CD4$^+$ T cells was significantly increased in male patients with severe compared to mild asthma (mean frequency 27% *versus* 12%; $P < 0.05$) (Figure S3I; and Table S2K). Notably, we analyzed published single-cell RNA-seq datasets[46–49] of BAL CD4$^+$ T cells from healthy controls and observed that the mean frequency of *GZMB*-expressing CD4$^+$ T cells in healthy BAL was decreased (9%) in comparison to our data (Figure S3I; and Table S2K). We also assessed the levels of Granzyme B, Granzyme A, CCL3 and CCL4 in BAL supernatants from matched patients by multiplex ELISA. However, we did not observe significant differences between disease groups (Figure S3J; and Table S1G), likely due to fact that other immune cell types like $CD8^+$ T cells and NK cells may also release these molecules.

Next, to determine potential relationship between the $CD103^+$ T_{RM} and $CD103^-$ T_{RM} subsets, we performed single-cell trajectory analysis of all airway $CD4^+$ T cells (Figure 3J) and a specific analysis of only T_{CM} and T_{RM} subsets (Figure S3K), which pointed to a transitional path originating from the T_{CM} cluster towards the $CD103^+$ T_{RM} cluster through the $CD103^-$ T_{RM} cluster as an intermediate population (Figure 3J; and Figure S3K). Additionally, TCR β-chain sequencing analysis of bulk populations of $CD103^+$ T_{RM}, $CD103^-$ T_{RM}, and non-T_{RM} subsets showed that the clonal repertoire of $CD103^+$ T_{RM} cells was significantly less diverse when compared to $CD103^-$ T_{RM} and non-T_{RM} clonotypes ($P < 0.01$ and $P < 0.001$) (Figure 3K; and Table S4B). Importantly, we observed that a large number of clonotypes from the $CD103^+$ T_{RM} subset were shared with the $CD103^-$ T_{RM} subset, suggesting that $CD103^+$ T_{RM} cells are clonally related to $CD103^-$ T_{RM} cells (Figure 3L; Figure S3L; and Table S4C). Overall, our single-cell transcriptomic analysis indicates that $CD103^+$ T_{RM} cells in the airways of asthmatic patients exhibit a T_H1-like phenotype with increased TCR activation, cytotoxicity, and pro-inflammatory effector properties.

Molecules that restrain T cell activation and effector functions are reduced in severe asthma

To determine qualitative differences in airway $CD4^+$ T cell subsets that are associated with asthma severity in both males and females, we performed independent single-cell differential gene expression analysis (scDGEA) of $CD4^+$ T cells from severe *versus* mild asthmatics for each sex (Figure 4A; and Table S2L) and per subset (Figure S4A; and Tables S2L and S2M). Overall, we observed that the most differentially expressed genes increased in severe asthma were significantly enriched in male patients, especially those linked to cytotoxicity (*GZMB*, *GZMH*, *ZNF683*, *HOPX*, *CCL4*) (Figure 4A; and Table S2L). Cluster-specific analysis showed that these cytotoxicity genes were differentially expressed only in the $CD103^+$ T_{RM} subset (Figure S4A; and Table S2L). While overall GSEA for cytotoxic signature genes showed significant enrichment in severe asthmatics, especially males, these observations were not confirmed at individual level when performing GSVA, likely due to a limited sample size and heterogeneity among the study participants (Figure S4B; and Table S2H). This finding suggests that although the $CD103^+$ T_{RM} subset was enriched in genes linked to TCR signaling and cytotoxicity, these features were not significantly different when comparing the $CD103^+$ T_{RM} subset from either males *versus* females or severe asthmatics *versus* mild asthmatics (Figures S4B and S4C; and Table S2H).

Interestingly, in both males and females with severe asthma, most $CD4^+$ T cell subsets including the T_{RM} subsets showed the highest significant reduction in the expression of several transcripts encoding for molecules known to dampen TCR signaling and effector functions in T cells (CREM, DUSP1, DUSP2, DUSP4, TNFAIP3)[77–81] (Figure 4B). One of the most downregulated differentially expressed genes is *CREM* (cyclic AMP responsive element modulatory), encoding for a transcription factor known to repress promoters of inflammatory cytokine genes like *IL2*, *IL13*, *IL4* and to dampen type 2 inflammation in murine asthma models.[79] Other transcripts with reduced expression in severe asthma encode for several members of the dual specificity phosphatase (DUSP) family proteins: DUSP1, a glucocorticoid responsive molecule that is known to inhibit activity of mitogen-activated protein kinases (MAPKs) that trigger cytokine production in immune cells;[77,82–84] DUSP2, which catalyzes dephosphorylation of STAT3 and inhibits T_H17 differentiation and inflammation;[77,85] and DUSP4, which dephosphorylates STAT5 and negatively regulates IL-2 signaling and T cell proliferation.[77,86] Lastly, TNFAIP3 is known to negatively regulate NFkB signaling, which is involved in T cell activation and effector function.[87,88] GSEA as well as single-sample GSVA confirmed negative enrichment for the immunoregulatory cAMP signaling pathway[89] in multiple $CD4^+$ T cell subsets from both male and female patients with severe asthma (Figure 4C-E; and Tables S2H and S3A).

Finally, one of the most significantly increased transcripts in many clusters in severe asthmatics, in both males and females, was *FKBP5*, a steroid-responsive gene, which encodes for the FK506 binding protein 5 (FKBP5)[90–92] (Figure 4B). As expected, this gene was significantly increased in the $CD103^+$ T_{RM} subset from severe asthmatics on OCS and biologics (Figures S3E and S3F). In severe asthmatics, cells in the T_{FH} cluster showed reduced expression of transcripts encoding for molecules linked to inhibitory function like *PD-1*, *TIM-3*, *LAG-3*, and *TIGIT*, which suggested the potential for unrestrained activity of airway T_{FH} cells in severe asthma[93] (Figure 4F). T_{REG} cells from severe asthmatics had significantly reduced levels of transcripts encoding for AP-1 family of transcription factors (*JUNB*, *JUN*, *FOS*, *FOSB*) that have been shown to be important for its suppressive functions[94,95] (Figure 4F). Overall, our analysis highlights the molecular properties of airway $CD4^+$ T cell subsets that can potentially trigger their unrestrained activation as well as confer resistance to corticosteroids in severe asthma.

Non-T_H2 pro-inflammatory cytokines are expressed by airway $CD4^+$ T cells from severe asthmatics

To examine the effector potential of airway $CD4^+$ T cells from patients with mild and severe asthma, we stimulated, *ex vivo,* a fraction of BAL cells with phorbol 12-myristate 13-acetate (PMA) and Ionomycin for 2 hours, and performed single-cell RNA-sequencing on over 35,000 sorted $CD4^+$ T cells (Figure S5A; and Table S2B). scDGEA between resting and stimulated $CD4^+$ T cells (Table S2N), as well as between stimulated cells from mild and severe asthmatic patients for each sex (Figure 5A; and Tables S2O and S2P), revealed several hundred transcripts linked to T cell effector function (Tables S2N and S3C). Transcripts linked to T_{RM} markers (*ITGAE, ITGA1*) (Figure 5B) were downregulated following stimulation, which prevented reliable identification of the T_{RM} subsets in stimulated datasets (Figure 5B). As expected, transcripts encoding for chemokines known to be released by cytotoxic $CD4^+$ T cells like CCL3, CCL4, and CCL5 [61,96–98] showed increased expression in stimulated airway $CD4^+$ T cells from patients with severe asthma compared to mild asthma (Figures 5A and 5B). These chemokines play key roles in the recruitment of several immune cell types expressing C-C chemokine receptor 1(CCR1), CCR3, CCR5, like neutrophils, monocytes, macrophages, NK cells, and T cell subsets,[99] which have the potential to drive airway inflammation and remodeling.[100,101]

Other transcripts upregulated by stimulation encode for molecules associated with T_H1 effector (*IFNG, TNF, FASLG, XCL1, XCL2*), and pro-fibrotic (*LIGHT, AREG, TGFB1*) properties (Figures 5A and 5B; and Table S2N). Although T_H2 and T_H17 cytokine transcripts were observed in stimulated airway $CD4^+$ T cells, only a relatively small fraction of cells was expressing *IL4, IL5, IL13, and IL17A* transcripts (3%, 2%, 16%, and 8%, respectively) and they were significantly reduced in patients with severe asthma compared to mild asthma (Figure 5B; and Table S2O). However, several other pro-inflammatory non-T_H2 cytokine transcripts were expressed by a larger fraction of airway $CD4^+$ T cells (*TNF* (80%), *CSF2* (40%), *CCL20* (50%) and *IL21* (23%)) (Figure 5B; and Tables S2N and S2O). Together, these data from stimulated cells suggests that the effector potential of airway $CD4^+$ T cells is not fully curtailed by high-dose corticosteroid treatment and that non-T_H2 cytokines may contribute to the pathogenesis of severe asthma.

To further explore the effector molecules expressed by cytotoxic $CD4^+$ T cells present in the airways, we examined the co-expression of cytokine transcripts specifically in *GZMB*-expressing cells, as *GZMB* is a canonical cytotoxicity-associated marker gene (Figures S5B and S5C; and Tables S2N, S2O, and S2Q). scDGEA between *GZMB*$^+$ versus *GZMB*$^-$ cells revealed over 1000 differentially expressed genes, among which we found transcripts encoding for cytotoxic molecules (GZMA, GZMH), and several pro-inflammatory cytokines and chemokines (CCL3, CCL4, CCL5, CCL20, TNF, IFN-γ, CSF2, IL21, LIGHT, TGFB1), known to contribute to airway inflammation, fibrosis, and remodeling; in part through regulating activity of fibroblasts and smooth muscle cells[50,70,71,102–111] (Figures 5C-E; Figure S5D; and Tables S2Q, S2R and S2S). These data suggest that cytotoxic $CD4^+$ T_{RM} cells, besides their potential for direct killing of target cells, can also express pro-inflammatory molecules, which may play an important role in sustaining airway inflammation and remodeling. To address the technical limitation in accurately classifying T_{RM} cells in stimulated $CD4^+$ T cells and to confirm their effector potential, we isolated specific $CD4^+$ T_{RM} cell populations from *ex vivo* stimulated BAL cells by flow cytometry and examined their bulk RNA-seq profile. As expected, stimulated cells from the $CD103^+$ T_{RM} subset expressed high levels of transcripts encoding for cytotoxicity-associated molecules (GZMB, GZMA, GZMH), pro-inflammatory chemokines (CCL3, CCL4, CCL5), and cytokines (TNF, IFN-γ, CSF-2, IL-21, IL-17A, IL-23A, IL-2, IL-13, LIGHT) (Figures S5E and S5F; and Tables S4D and S4E). Overall, these findings supported the existence of a population of $CD4^+$ T_{RM} cells with features of cytotoxicity and polyfunctionality in BAL samples collected from severe asthmatics.

DISCUSSION

Here, we report on the single-cell transcriptomes from purified $CD4^+$ T cells isolated from the airways of patients with severe and mild asthma. This unbiased approach led to the discovery of a cytotoxic $CD4^+$ T_{RM} cell subset in severe asthma that we hypothesize is critical in driving airway inflammation and remodeling in a specific subgroup *i.e.*, males with severe asthma, where we found a striking increase in the proportions of a $CD4^+$ T_{RM} subset ($CD103^+$ T_{RM} cells) with cytotoxic properties in the airways.

Asthma is now acknowledged to be a heterogeneous state with numerous clinical phenotypes that show considerable diversity. The current prevailing paradigm is to stratify asthma endotypes as either type 2 (T2)-high or T2-low.[112] However, recent findings from the analysis of clinical and pathophysiological characteristics between patients classified as T2-high and T2-low from the WATCH study demonstrated that when properly characterized, asthma is an overwhelmingly T2 state (93%),[14] supporting that the T2 paradigm by itself cannot explain the diversity of asthma at a pathophysiological level, instead other pathways driven by for example cytotoxic $CD103^+CD4^+$ T_{RM} cells may define endotypes underlying diverse phenotypes of severe asthma.[14,113] For instance, the WATCH cohort study defined distinct clinical phenotypes of severe asthma stratified by age of asthma onset and sex.[62] These findings confirmed a previously poorly recognized phenotype of severe asthma, adult-onset male severe asthmatics, characterized by numerous adverse clinical features including worse lung function despite short disease duration, higher peripheral blood eosinophilia, higher exhaled nitric oxide, greater oral corticosteroid dependency, and little of the typical psychophysiological comorbidities seen in difficult-to-treat asthma.[62] This clinical phenotype has been previously shown in other studies though attracted little focus hitherto.[114–117]

In the present study, we identified potential endotypic features, *i.e.* cytotoxic $CD103^+CD4^+$ T_{RM} cells, that underpin such clinical phenotype. The $CD103^+CD4^+$ T_{RM} cells also displayed a unique pro-inflammatory cytokine and chemokine signature, highly enriched in transcripts encoding molecules (*e.g.* Granzymes, CCL3, CCL4, LIGHT, TNF, IL-21) that drive inflammation, cell death, and fibrosis.[71,108,118,119] Because T_{RM} cells are a long-term resident population in the airways, they have the potential for sustained interaction with airway structural cells and thus the products they release are likely to promote persistent airway inflammation and remodeling in severe asthma.

While T_H2 cells and, to a lesser extent, T_H17 and T_H1 cells have been implicated in asthma pathogenesis and therapies targeting T_H2 cytokines are beneficial for some patients with asthma, the role of cytotoxic $CD4^+$ T cells in severe asthma pathogenesis has not been previously described. Cytotoxic $CD4^+$ T cell responses have been reported in certain viral infections such as human cytomegalovirus, human immunodeficiency virus, dengue virus, hepatitis C virus, influenza virus, and, more recently, with SARS-CoV2 virus.[96,120–130] Outside the context of viral infections, reports from studies employing single-cell genomics have shown an increased number of cytotoxic $CD4^+$ T cells in patients with autoimmune diseases such as rheumatoid arthritis[131] and multiple sclerosis.[132] These cells expressed high levels of pro-inflammatory cytokines and are hypothesized to drive disease pathogenesis. Most importantly, an increased number of cytotoxic $CD4^+$ T cells has been observed in several steroid-resistant diseases with pronounced organ fibrosis such as systemic sclerosis,[100] idiopathic pulmonary fibrosis,[133] IgG4 disease,[101] and graft versus host disease,[134] suggesting that cytokines and other currently uncharacterized factors released by cytotoxic $CD4^+$ T_{RM} cells are likely to play a significant role in promoting clinical hallmarks of severe asthma such as persistent inflammation, fibrosis, and airway remodeling. Based on previous research showing that sustained T cell activation through TCR engagement drives the differentiation of $CD4^+$ T cells into CD4 cytotoxic T lymphocytes (CD4 CTLs),[135] we hypothesize that, in the airways of severe asthmatics,

$CD103^+CD4^+$ T_{RM} cells with cytotoxic features are likely to represent cells that received chronic TCR stimulation.

Furthermore, our findings support that airway $CD4^+$ T_{RM} cells display a T_H1-like pro-inflammatory potential namely by secreting CCL3, CCL4, and CCL5, pro-inflammatory chemokines that are also linked to viral airway infections and virus-triggered asthma exacerbations.[136,137] Their cognitive receptor, mainly CCR5, has been recently associated with $CD4^+$ T_{RM} cells and associated with worsening of lung function in asthmatic patients.[29] CCR5 inhibition in a murine model of type-1 allergic lung inflammation showed a drastic reduction of airway hyperresponsiveness and inflammation.[138,139] Based on this finding, we speculate that, in severe asthma, especially males, the sustained release of CCL3, CCL4, and CCL5 by activated $CD4^+$ T_{RM} cells triggers a pro-inflammatory milieu that can worsen airway inflammation and remodeling in severe asthma.

In summary, our findings support a potentially important role for cytotoxic $CD4^+$ T_{RM} cells in driving disease pathogenesis and, more specifically, in a subgroup of severe asthmatics, and thus may represent an attractive target for therapeutic development. Our work also potentially expands the portfolio of treatable traits that have gained increasing attention in severe asthma management,[140] with the intriguing concept that patient sex and airway $CD4^+$ T cell profile may help guide disease assessment, prognosis and treatment.

Limitations of the study

Future studies are required to address the nature of antigens recognized by cytotoxic $CD4^+$ T_{RM} cells in severe asthma, as it is unclear if these antigens are allergens, pathogens, or potential autoantigens. Determining the specificity of cytotoxic $CD4^+$ T_{RM} is likely to provide insights into mechanisms that induce and sustain their generation and maintenance in the airways of severe asthmatics. Furthermore, studies in model organisms are required to functionally establish whether cytotoxic $CD4^+$ T cells and the pro-inflammatory molecules they produce are capable of initiating and maintaining persistent airway inflammation and remodeling.

In addition, as severe asthma is a heterogeneous disease, it will be essential to confirm the association between cytotoxic $CD4^+$ T_{RM} cells and specific phenotypes of severe asthma in large-scale studies of airway $CD4^+$ T cells from well-characterized cohorts of patients with severe and mild asthma across different age groups, ethnicities, and diverse geographical locations. Longitudinal studies are required to define whether severe asthmatics with high frequency of cytotoxic $CD103^+CD4^+$ T_{RM} cells are associated with more adverse long-term outcomes. In particular, future studies should assess associations of $CD103^+CD4^+$ T_{RM} cells with biologics treatment outcomes to establish their potential as biomarkers of biologics responsiveness. Such studies should also monitor the frequency of $CD103^+CD4^+$ T_{RM} cells in the airways before and after biologics treatment to determine if their frequency can be modulated by currently available biologics therapies.

Finally, as sex hormones fluctuate across an individuals' lifespan with important consequences on severe asthma pathogenesis as well as on treatment efficacy[141,142], a larger study that examines the influence of sex and sex hormones on the immune landscape of airway T cells in severe asthmatics is required.

STAR METHODS

RESOURCE AVAILABILITY

Lead contact—Further information and requests for resources and reagents should be directed to and will be fulfilled by Lead Contact, Grégory Seumois (gregory@lji.org).

Materials availability—This study did not generate new unique reagents.

Data and code availability

- Sequencing data are available from NCBI as Gene Expression Omnibus, SuperSeries accession number GSE181711 (Subseries: GSE181709 for bulk RNA-seq data and GSE181710 for single-cell RNA-seq data).
- Scripts are available in our repository on GitHub (https://github.com/vijaybioinfo/ASTHMA_AIRWAYS_2021).
- Any additional information required to reanalyze the data reported in this paper is available from the lead contact upon request.

EXPERIMENTAL MODEL AND STUDY PARTICIPANT DETAILS

Patient recruitment, ethical approval, and characteristics—Study participants diagnosed with asthma were recruited into the National Institutes of Health Epigenetics of Severe Asthma study (n=193) from established cohorts of patients (United Kingdom (UK)): the Wessex AsThma CoHort of difficult asthma (WATCH) at University Hospital Southampton Foundation Trust UK[41] (n=501) consisting of patients with severe/difficult-to treat asthma (GINA management steps 4 and 5[43]) and the Isle of Wight Whole Population Birth Cohort (IOWBC) at the David Hide Asthma and Allergy Research Centre, Isle of Wight, UK[143] (n=1,456), along with clinic/community recruitment on the Isle of Wight, UK, of mild asthma patients (GINA management steps 1 and 2, with a small proportion with step 3, see Table S1A). Adherence to treatment in these patients was clinically assessed using a Medicines Possession Ratio (MPR) threshold of acceptable. This study received approval from the South Central Hampshire B – Southampton Research Ethics Committee, UK (REC reference: 18/SC/0105) and from the La Jolla Institute for Immunology Institutional Review Board (IRB VD-156–1118, La Jolla Institute for Immunology, La Jolla, USA). Written informed consent was obtained from all study participants. Thirty patients were included in this study based on the identification of clinically severe airways disease and on the safety criteria for bronchoscopy being satisfied. Briefly, study participants underwent an extensive clinical characterization process including detailed clinical, health and disease-related questionnaires, anthropometry, and lung function testing (Table S1A). Patients with mild (GINA 1 to 3, n=14) and severe asthma (GINA 4 and 5, n=16) underwent fiberoptic bronchoscopy for collection of BAL samples. Mild asthmatic patients were treated with inhaled bronchodilators alone (Salbutamol 200 μg as required) (n=4) and/or with low to medium dose of inhaled corticosteroids (400 to 800 μg/day beclomethasone dipropionate

(BDP) equivalent, n=10). Conversely, all severe asthmatic patients were treated with high dose inhaled corticosteroids (1,200 to 2,000 µg/day BDP equivalent) and second controller medication (n=14), and/or on daily maintenance oral steroids (n=5) and/or biological monoclonal antibody treatment (Omalizumab (anti-IgE), n=2; Mepolizumab (anti-IL-5), n=7) (details provided in Table S1A).

METHOD DETAILS

BAL samples processing—BAL fluid was obtained by instilling a total volume of 120 ml of warm 0.9% saline in small aliquots (initially 40 ml followed by 20 ml, holding for 10 seconds each time) into the right upper lobe segments using a fiberoptic bronchoscope procedure (n = 30). Aliquots were pooled together and collected as 1 sample with immediate storage on ice. The median recovery of BAL volume was 53 ml (Inter-quartile range: 24–60 ml). RNAse inhibitor (v:v 1:1000, Takara Bio) and protease inhibitor (v:v 1:50; Sigma Aldrich) were immediately added to BAL collected. BAL was then filtered within 30 minutes with a 100 µm BD cell strainer and centrifugated at 300 x g for 10 minutes at 4°C. Cellular fractions were resuspended in 1 ml of phosphate buffer solution (PBS) with RNAse inhibitor (v:v 1:100). Two Cytospin slides were generated with 70 µl of cell suspension using a Shandon Cytospin 2 and stained using rapid Romanowsky (Diff-Quick) stain to obtain differential cell counts and to ascertain the volume of squamous cell contamination.[41] Samples were centrifugated once more at 300 x g for 10 minutes at 4˚C. Supernatants were discarded and cell pellets resuspended into freezing media (50% human decomplemented AB Serum (Sigma Aldrich), 40% complete Gibco Roswell Park Memorial Institute (RPMI) medium (ThermoFisher Scientific) complemented with 10% heat-inactivated fetal bovine serum (FBS) (Sigma Aldrich, 10% DMSO (Sigma Aldrich), and 5 µl of RNAse inhibitor, before slow cryopreserving at −80°C as described previously.[58] All BAL samples were collected and cryopreserved in the UK, stored in liquid nitrogen tanks, and sent later to La Jolla Institute for Immunology for processing.

Flow cytometry of cryopreserved BAL cellular samples—Cryopreserved samples were thawed, and cells were transferred first to 1 ml of cold heat-inactivated FBS and then quickly diluted up to 10 ml with complete TCM medium (Gibco Iscove's Modified Dulbecco's Medium (IMDM) with 5% FBS and 2% human serum; ThermoFisher Scientific). Samples were centrifugated at 250 x g for 5 minutes at room temperature. Supernatants were discarded and cells resuspended in appropriate volume of MACS buffer (PBS, 2 mM EDTA, 2% heat-inactivated FBS) to reach 2 million cells per ml. Around 25% of the sample or maximum of 500,000 cells were separated for stimulation assays. Remaining cells were centrifuged at 400 x g for 5 minutes at room temperature, supernatant was discarded, and cells resuspended in 200 µl of MACS buffer complemented with 1% RNAse inhibitor. All samples (resting or after stimulation) were stained following a standard procedure previously described.[58] Briefly, 200 µl cell suspensions were first incubated with 20 µl of FcgR blocking solution (Miltenyi Biotec) for 15 minutes on ice, and subsequently stained with the following combination of fluorescently-conjugated antibodies: anti-CD45-Alexa Fluor 700 (2D1; BioLegend), anti-CD3-APC-Cy7 (SK7; BioLegend), anti-CD8a-BV570 (RPA-T8; BioLegend), anti-CD4-BV510 (RPA-T4; BioLegend), anti-CD357(GITR)-BV711 (108–17; BioLegend), anti-CD185(CXCR5)-BV421 (RF8B2; BD

Biosciences), anti-CD25-BB515 (2A3; BD Biosciences), anti-CD127-APC (eBioRDR5; eBioscience), anti-CD69-BV605 (FN50; BioLegend) and anti-CD103-PE-Cy7 (Ber-ACT8; BioLegend). The Brilliant Stain Buffer Plus (BD Biosciences) was also added to the antibody mix as recommended. For a fraction of the samples, the DNA-oligonucleotide conjugated anti-CD103 (TotalSeq-A0145; Ber-ACT8; BioLegend) and anti-CD69 antibodies (TotalSeq-A0146; FN50; BioLegend) were also added. After 20 minutes incubation in the dark, on ice, cells were washed once with 5 mL of ice-cold MACS buffer, centrifugated at 400 x g for 5 minutes at room temperature (RT), resuspended in 250 µl MACS buffer with RNAse inhibitor (10%), and brought to flow cytometry for immunophenotyping analyses and sorting. Live and dead cells were discriminated using propidium iodide (PI, 1:200 vol:vol). All stained samples were analyzed using BD FACSAria Fusion Cell Sorter (BD Biosciences) and FlowJo software (v10.7.1).

Stimulation assays—Maximum 25% of BAL samples and no more than 500,000 cells from each BAL sample were stimulated *ex vivo* in 1 ml of complete TCM medium complemented with PMA (final 20 nM, phorbol-12-myristate-13-acetate) and ionomycin (final 1 µM; Sigma Aldrich) for 2 hours in a cell culture incubator at 37˚C and 5% CO_2. Samples were then processed and stained for flow-cytometry analysis and sorting as described here above.

Cell isolation for bulk and single-cell RNA-seq assay—For bulk RNA-seq assays, cells of interest were directly collected by sorting 400 cells into 0.2 ml PCR tubes (low-retention, Axygen) containing 8 µl of ice-cold lysis buffer (Triton X-100 [0.1%, Sigma-Aldrich] and 1% RNase inhibitor [Takara Bio]). Once collected, tubes were vortexed for 10 seconds, spun for 1 minute at 3000 x g and directly stored at −80˚C. For single-cell RNA-seq assays (10x Genomics), 1,000 to 2,000 airway $CD4^+$ T cells were sorted per BAL sample directly in low retention and sterile ice-cold 1.5 ml collection tubes containing 500 µl of PBS:FBS (1:1 vol:vol) with RNAse inhibitor (1:100). Samples were batched in groups of 5 to 6 donors with similar disease status. Samples were also separated based on stimulation. In total, we performed 6 sorting experiments (see Table S1C). Collection tubes with ~10,000 to 20,000 sorted $CD4^+$ T cells were inverted a few times, ice-cold PBS was added to reach a volume of 1,400 µl, and tubes were centrifuged for 5 minutes at 600 x g and 4˚C. Supernatant was removed with caution, leaving a volume of around 10 µl. Pellets were then resuspended with 35 µl of 10X Genomics resuspension buffer (0.22 µm filtered ice-cold PBS supplemented with ultra-pure bovine serum albumin (0.04%, Sigma-Aldrich). 40 µl of cell suspension were transferred to an 8 PCR-tube strip for downstream steps as per manufacturer's instructions (10x Genomics).

Bulk RNA library preparation for sequencing—For full-length bulk transcriptome analyses, we used the Smart-seq2 protocol (adapted for samples with small cell numbers).[144–146] Briefly, RNA was captured using oligo-poly(dT)-3' primers and reverse transcription was performed using 5'-template switching oligos (LNA technologies, Exicon). cDNA was pre-amplified by PCR cycle for 20 cycles. Amplified cDNA was cleaned by applying a double size purification (0.6 vol:vol and 0.8 vol:vol with Ampure-XP magnetic beads (Beckman Coulter)). After quantification and quality assessment using capillary electrophoresis (Fragment analyzer, Advance analytical), 0.5 ng of pre-amplified cDNA was used to generate indexed Illumina libraries (Nextera XT library preparation kit, Illumina). Every sample was quality checked for fragment size by capillary electrophoresis (Fragment analyzer, Advance analytical) and quantified (Picogreen, Thermofisher). No libraries failed our quality control check steps and therefore were pooled at equal molar concentration before loading on the NovaSeq 6000 Illumina sequencing platform. Every library was sequenced to reach a minimum of 15 million 100 × 100 bp pair-ended sequencing reads (S4 flowcell 200 cycle v1.0, Xp workflow; Illumina).

10x Genomics single-cell RNA library preparation for sequencing—Samples were processed using 10X Genomics 3v3.0 single cell gene expression profiling chemistry as per manufacturer's recommendations; after droplet generation, and in-droplet based reverse transcription, cDNA was amplified by PCR for 11 cycles and gene expression library preparation followed. After quantification, equal molar concentration of each library was pooled and sequenced using the NovaSeq6000 Illumina sequencing platform to obtain 28- and 100-bp paired-end reads using the following read length: read 1, 100 cycles; read 2, 100 cycles; i7 index, 8 cycles and i5 index 8 cycles. Each library was sequenced aiming at a minimum mean sequencing depth of 87,000 reads per cell. For samples stained with DNA-oligo-conjugated-cell-surface antibodies (TotalSeq-A, Biolegend), amplified DNA generated from antibody-DNA oligos was separated from transcriptomic cDNA based on size-selection following amplification. Antibody-DNA amplified fragments are less than 300 bp. Library preparation was followed in accordance with the manufacturer's recommendations. TotalSeq libraries were quantified and sequenced in the same manner as the gene expression libraries, as described above. Each library was sequenced aiming for 5,000 reads per cell.

Genotyping—For each patient, genomic DNA was isolated from PBMC using the DNeasy Blood and Tissue Kit (Qiagen) and utilized for genotyping using the Infinium Multi-Ethnic Global-8 Kit (Illumina) following the manufacturer's instructions. Chip-arrays were run on an Illumina iScan System using the University of California - San Diego, Institute of Genomic Medicine. Raw data from the genotyping analysis, data quality assessment and SNPs identification were performed as previously described.[58]

Bulk RNA-seq analysis—Bulk RNA-seq data were mapped against the hg19 genome reference using our in-house pipeline (https://github.com/ndu-UCSD/LJI_RNA_SEQ_PIPELINE_V2). Briefly, FASTQ data from sequencing was merged and filtered using fastp (v0.20.1), reads were aligned with the STAR aligner (v2.7.3a), followed by further processing with samtools (v0.1.19–44428cd), bamCoverage (v3.3.1), and Qualimap (v.2.2.2-dev). Raw and transcripts per million reads (TPM) counts were taken from STAR's BAM aligned output.

To identify genes expressed differentially between groups, we performed negative binomial tests for paired comparisons by employing DESeq2[147] (v1.16.1) with default parameters and batch and sex as a covariate. We considered genes to be expressed differentially by any comparison when the DESeq2 analysis resulted in a Benjamini-Hochberg–adjusted *P*-value of less than 0.01 and a $\log_2$ fold change of at least 1.

TCR-seq analysis—To profile the bulk data's TCR repertoire, FASTQ files per bulk RNA-seq libraries were fed to the MiXCR algorithm[148] (v2.1.10, RepSeq.IO v1.2.11, MiLib v1.8.3). The TCR sharing was determined using the β chain from MiXCR's *clonalSequence* per donor when comparing cell types. This TCR sharing was displayed using the ComplexUpset package (v1.3.3).

TCR diversity indexes calculation.: Inverse Simpson and Shannon-Wiener diversity indexes were calculated with CalcDiversityStats module of vdjtools software (v1.2.1, default settings)[149] taking TCR β amino acid and nucleotide sequences, TRB clone counts, and VDJ gene information per donor of sorted T_{RM} bulk TCR samples previously analyzed with MiXCR software (Table S4B).

Integration analysis of published BAL healthy datasets—To determine the proportions of $CD4^+CD69^+CD103^+$ T_{RM} and $CD4^+CD69^+CD103^-$ T_{RM} cells by flow cytometry in BAL healthy donors (Figure 2H), we used published data from Diniz, *et al.,*[44] Tang, *et al.,*[45] and Camiolo, *et al.* (GSE136587)[29]. We retrieved 29 healthy donors from these published datasets.

To determine the frequency of *GZMB*-expressing $CD4^+$ T cells in single-cell RNA-seq BAL healthy datasets (Figure S3I), healthy donors were directly collected from Liao, *et al.* (GSE145926);[46] Grant, *et al.* (GSE155249);[47] Morse, *et al.* (GSE128033);[48] and Mould, *et al.* (GSE151928)[49] datasets. Author's labels were used to analyze $CD4^+$ cells from these datasets, except Morse, *et al.* for which we used $CD3D^+$ cells. We retrieved 17 healthy donors from these published datasets.

Single-cell RNA-Seq analysis

Analysis of 3' transcriptome of single-cell from 10x Genomics platform.: Raw data was processed as previously described,[22,33,61] merging multiple sequencing runs using Cell Ranger's *count* function (Table S2B), then aggregating multiple cell types with *aggr* (v3.1.0).[150]

Doublet cell filtering and donor labeling.: Barcoded single-cell RNA-seq was demultiplexed patient-wise using Demuxlet[151] with the following parameters: alpha=0, 0.5 and --geno-error=0.05. Each cell was assigned a donor ID or marked as a doublet. Cells called as doublet by Demuxlet were removed from downstream analyses. We did not observe major changes in singlets/doublets proportions between the different 10x Genomics libraries, suggesting optimal processing of cells during 10x (Gel Bead-In emulsions) GEM generation and downstream steps. All downstream analyses were performed using cells labelled as singlets.

$CD4^+$ cells selection from stimulated $CD3^+$ library.: Differential gene expression analysis was performed between filtered $CD4^+$ $CD8B^-$ and $CD4^-$ $CD8B^+$ cells from the $CD3^+$ library, and differentially expressed genes were used for clustering. Genes were selected with a Benjamini-Hochberg adjusted *P*-value less than 0.05, $\log_2$ |Fold Change| higher than 2 and sex-related genes were excluded (*RPS4Y1, XIST, SPRY1, DDX3Y*). Two clusters were identified correlating with the CD4 and CD8 T cell types from which only the $CD4^+$ was taken for downstream analysis of stimulated data.

Transcriptome-based clustering analysis.: The merged data was transferred to the R statistical environment for analysis. Unbiased clustering analysis was performed using Seurat (v3.0.2).[152] A first round of analysis was run and single-cell transcriptomes not meeting quality control thresholds (see below) as well as a cluster of contaminating cells characterized by a strong monocyte/macrophage signature were eliminated from the second round of analysis. Only cells expressing between 200 and 6,000 genes, less than 30,000 total unique molecule identifier (UMI) content, and less than 15% of reads mapping to mitochondria genome were included. Only genes expressed in at least 0.1% of the cells were included in the analysis. Expression counts were then log-normalized and scaled (by a factor of 10,000) per cell. Variable genes were detected with the VST method and the top highly expressed (UMI mean greater than 0.01) genes representing 15% of the cumulative variance were selected for cluster analysis. Transcriptomic data from each cell was then further scaled by regressing the number of UMI-detected and the percentage of mitochondrial reads. Principal component analysis (PCA) was then run on the variable genes, and the first 20 principal components were selected for downstream analyses based on the standard deviation of PCs ("elbow plot") (Figure S1C). Cells were clustered using Seurat's functions *FindNeighbors* and *FindClusters* with a resolution of 0.4. We performed downstream analyses excluding a cluster ($T_{APOPTOSIS}$) (< 2% of airway $CD4^+$ T cells) enriched in apoptosis signature genes (as reported by GSEA) and interpreted as a technical artefact (Figure S1F).

Gene-set score calculation and gene set enrichment analysis (GSEA).: Signature scores were calculated with *AddModuleScore* function from Seurat with default settings. The score is derived from the mean of the gene list after subtracting a background expression calculated from a random list of genes (same size as the gene set). The normalized GSEA enrichment score was calculated using *fgsea* (v 1.10.1) in R with the signal-to-noise ratio as a metric.[153] Default parameters were used except minSize = 3 and maxSize = 500. Gene set lists are in Table S3A.

Gene-set variation analysis (GSVA).: To determine enrichment scores for predefined lists of genes in individual samples, we performed GSVA.[154] Single-cell GSVA was performed using the *scgsva* function with default parameters, utilizing the scGSVA package (v0.0.14, available at https://github.com/guokai8/scGSVA). To calculate the enrichment scores per donor for a specific cluster of cells, i.e. $CD103^+$ T_{RM} cells, the arithmetic mean of all single-cell enrichment scores was computed.

Pathway analysis.: For unbiased pathway enrichment analysis of differentially expressed genes as well as network and upstream regulator analysis shown in Figure 3C, Figure S3D, and Table S3B, we used the IPA software (IPA, QIAGEN Redwood City, www.qiagen.com/ingenuity). Relevant pathways were selected using a filter based on significance index (P value [-log10]) > 2 and ordered based on z score. For the figure, any multiple pathways with similar enriched genes were summarized into one representative pathway labelled based on gene functions. For Table S3C, we used the clusterProfiler package[155] (v4.6.2) in R and performed enrichment analysis of gene ontology (GO) categories using the *enrichGO* function taking as "genes" highly differentially expressed genes (log2FC >= 2, padj < 0.05, stimulation *versus* resting condition comparison) and all differentially expressed genes (log2FC >= 0.25, padj < 0.05, stimulation *versus* resting condition comparison) as background (Table S3C). Default parameters were used except ont = "MF".

Protein expression analysis using DNA-oligo-antibody single-cell sequencing.: TotalSeq-A reads were analyzed based on recommendation provided by manufacturer (BioLegend).

Single-cell differential gene expression analysis.: Pairwise analyses were performed using the R package MAST (v 1.8.2)[156] with cellular detection rate (CDR) as a covariate, after normalizing the data to $\log_2$ counts per million ($\log_2$(CPM+1)). A gene was considered as differentially expressed if its Benjamini-Hochberg adjusted *P*-value was < 0.05 and $\log_2$ (|fold change|) was >0.25 (otherwise noted in legends). Cluster specific markers were determined by MAST using the Seurat function *FindAllMarkers* with default parameters. *Violin plots* represent the distribution of expression (based on a Gaussian Kernel density estimation model) of cells including cells with no expression. Violins are colored according to the percentage of cells expressing the transcript of interest.

Volcano plots represent the differentially expressed transcripts with the color showing the average expression ($\log_2$) derived from the group in which the gene is up-regulated and the size showing the difference in percentage of expressing cells between groups. Only transcripts present in > 25% of the total cells are shown in the volcano, but all the differentially expressed genes are shown in the corresponding supplementary tables. *Crater plots* are scatter plots that depict $\log_2$ (|fold change|) of expression for all transcripts from two distinct scDGEA comparisons, each comparison representing one axis. Every dot is a given transcript, with the size representing the average of both significance values [-$\log_{10}$ (adjusted *P*-value)] and the color representing the average level of expression for all cells analyzed.

Single-cell trajectory analysis.: Single-cell trajectory analysis was performed using Monocle 3 (v1.0.0, default settings).[157] Briefly, the method employed the number of unique molecular identifiers (UMIs) and the percentage of mitochondrial UMIs as the model formula, in addition to the most variable genes identified through Seurat analysis, to ensure consistency. Two different partitions were obtained using the *cluster_cells* function, followed by trajectory learning with *learn_graph* (minimal_branch_len=30). To visualize the cell pseudotime, the trajectory was projected onto the principal component analysis (PCA) and unified manifold approximation and projection (UMAP) generated from Seurat analysis. The T_{CM} cluster was selected as the root based on prior biological knowledge.

ELISA for protein quantification—Cytotoxic molecules (GZMA, GZMB) and pro-inflammatory cytokines (CCL3, CCL4) from BAL supernatants (> 100 mL) from mild and severe asthmatic patients were quantified using a multiplex ELISA assay (U-PLEX assay platform, Meso Scale Discovery), following the manufacturer's instructions. Total protein in the BAL supernatants was measured using the Pierce BCA technique (Pierce BCA Protein Assay Kit, Thermo Scientific) for normalization of protein concentrations.

QUANTIFICATION AND STATISTICAL ANALYSIS

Statistical analysis—For RNA-seq data analysis, statistical methods have been described here above. We used unpaired nonparametric T test (Mann-Whitney) for analysis between two groups, and unpaired non-parametric Kruskal-Wallis test for multiple comparisons (more than two groups) followed by Dunn's post-hoc test for correction. For correlation analysis with clinical features, as the data used was either ordinal and/or non-linearly distributed, we used Spearman correlation coefficients followed by Bonferroni-Hochberg correction. Correlation trendlines were drawn by simple linear regression. We used GraphPad Prism 9.0.1. All source data is detailed in Supplementary Tables.

Supplementary Material

Refer to Web version on PubMed Central for supplementary material.

ACKNOWLEDGMENTS

We thank Drs. C. Kim, D. Hinz and members of the flow cytometry core facility at La Jolla Institute for Immunology (LJI); and the members of the Vijayanand laboratory for scientific support. We also thank all donors for their charitable contribution to academic research. This work was supported by (*i*) NIH research grants R01HL114093 and U19-AI070535 (PV) and equipment grants (S10RR027366 - BD FACSAria II, and S10OD025052 - Illumina Novaseq 6000); (*ii*) the William K. Bowes Jr. Foundation (P.V.); (*iii*) and BioLegend – BioLegend Fellow (S.H-M.). The WATCH study is supported by the Southampton NIHR Biomedical Research Centre and the Southampton NIHR Clinical Research Facility which are funded by the NIHR and are a partnership between the University of Southampton and University Hospital Southampton NHS Foundation Trust.

Funding

This research was funded by the NIH.

INCLUSION AND DIVERSITY

We worked to ensure gender balance in the recruitment of human subjects. We worked to ensure that the study questionnaires were prepared in an inclusive way. One or more of the authors of this paper self-identifies as an underrepresented ethnic minority in their field of research or within their geographical location. One or more of the authors of this paper self-identifies as a gender minority in their field of research. One or more of the authors of this paper self-identifies as a member of the LGBTQIA+ community. We support inclusive, diverse, and equitable conduct of research.

REFERENCES

1. Dharmage SC, Perret JL, and Custovic A. (2019). Epidemiology of Asthma in Children and Adults. Front Pediatr 7, 246. 10.3389/fped.2019.00246. [PubMed: 31275909]
2. Hammad H, and Lambrecht BN (2021). The basic immunology of asthma. Cell 184, 2521–2522. 10.1016/j.cell.2021.04.019. [PubMed: 33930297]
3. León B, and Ballesteros-Tato A. (2021). Modulating Th2 Cell Immunity for the Treatment of Asthma. Frontiers in Immunology 12. 10.3389/fimmu.2021.637948.
4. Prevention., C.f.D.C.a. (2020). 2019 National Health Interview Survey data. U.S. Department of Health & Human Services. https://www.cdc.gov/asthma/nhis/2019/data.htm.
5. Hough KP, Curtiss ML, Blain TJ, Liu R-M, Trevor J, Deshane JS, and Thannickal VJ (2020). Airway Remodeling in Asthma. Frontiers in Medicine 7. 10.3389/fmed.2020.00191.

6. Lambrecht BN, Hammad H, and Fahy JV (2019). The Cytokines of Asthma. Immunity 50, 975–991. 10.1016/j.immuni.2019.03.018. [PubMed: 30995510]

7. Seumois G, Zapardiel-Gonzalo J, White B, Singh D, Schulten V, Dillon M, Hinz D, Broide DH, Sette A, Peters B, and Vijayanand P. (2016). Transcriptional Profiling of Th2 Cells Identifies Pathogenic Features Associated with Asthma. The Journal of Immunology 197, 655–664. 10.4049/jimmunol.1600397. [PubMed: 27271570]

8. Wadhwa R, Dua K, Adcock IM, Horvat JC, Kim RY, and Hansbro PM (2019). Cellular mechanisms underlying steroid-resistant asthma. European Respiratory Review 28, 190096. 10.1183/16000617.0096-2019.

9. Drazen JM (2012). Asthma: the paradox of heterogeneity. J Allergy Clin Immunol 129, 1200–1201. 10.1016/j.jaci.2012.03.026. [PubMed: 22541360]

10. Chung KF, Wenzel SE, Brozek JL, Bush A, Castro M, Sterk PJ, Adcock IM, Bateman ED, Bel EH, Bleecker ER, et al. (2014). International ERS/ATS guidelines on definition, evaluation and treatment of severe asthma. European Respiratory Journal 43, 343–373. 10.1183/09031936.00202013. [PubMed: 24337046]

11. Castro M, Corren J, Pavord ID, Maspero J, Wenzel S, Rabe KF, Busse WW, Ford L, Sher L, FitzGerald JM, et al. (2018). Dupilumab Efficacy and Safety in Moderate-to-Severe Uncontrolled Asthma. New England Journal of Medicine 378, 2486–2496. 10.1056/NEJMoa1804092. [PubMed: 29782217]

12. Ortega HG, Liu MC, Pavord ID, Brusselle GG, FitzGerald JM, Chetta A, Humbert M, Katz LE, Keene ON, Yancey SW, and Chanez P. (2014). Mepolizumab Treatment in Patients with Severe Eosinophilic Asthma. New England Journal of Medicine 371, 1198–1207. 10.1056/NEJMoa1403290. [PubMed: 25199059]

13. Humbert M, Taillé C, Mala L, Le Gros V, Just J, and Molimard M. (2018). Omalizumab effectiveness in patients with severe allergic asthma according to blood eosinophil count: the STELLAIR study. European Respiratory Journal 51, 1702523. 10.1183/13993003.02523-2017.

14. Rupani H, Kyyaly MA, Azim A, Abadalkareen R, Freeman A, Dennison P, Howarth P, Djukanovic R, Vijayanand P, Seumois G, et al. (2023). Comprehensive Characterization of Difficult-to-Treat Asthma Reveals Near Absence of T2-Low Status. J Allergy Clin Immunol Pract. 10.1016/j.jaip.2023.05.028.

15. Liu W, Liu S, Verma M, Zafar I, Good JT, Rollins D, Groshong S, Gorska MM, Martin RJ, and Alam R. (2017). Mechanism of TH2/TH17-predominant and neutrophilic TH2/TH17-low subtypes of asthma. Journal of Allergy and Clinical Immunology 139, 1548–1558.e1544. 10.1016/j.jaci.2016.08.032. [PubMed: 27702673]

16. Koch S, Sopel N, and Finotto S. (2017). Th9 and other IL-9-producing cells in allergic asthma. Seminars in Immunopathology 39, 55–68. 10.1007/s00281-016-0601-1. [PubMed: 27858144]

17. Zhou T, Huang X, Zhou Y, Ma J, Zhou M, Liu Y, Xiao L, Yuan J, Xie J, and Chen W. (2017). Associations between Th17-related inflammatory cytokines and asthma in adults: A Case-Control Study. Scientific Reports 7, 15502. 10.1038/s41598-017-15570-8. [PubMed: 29138487]

18. Cui J, Pazdziorko S, Miyashiro JS, Thakker P, Pelker JW, Declercq C, Jiao A, Gunn J, Mason L, Leonard JP, et al. (2005). TH1-mediated airway hyperresponsiveness independent of neutrophilic inflammation. J Allergy Clin Immunol 115, 309–315. 10.1016/j.jaci.2004.10.046. [PubMed: 15696086]

19. Sahoo A, Alekseev A, Tanaka K, Obertas L, Lerman B, Haymaker C, Clise-Dwyer K, McMurray JS, and Nurieva R. (2015). Batf is important for IL-4 expression in T follicular helper cells. Nature Communications 6, 7997. 10.1038/ncomms8997.

20. Bošnjak B, Kazemi S, Altenburger LM, Mokrović G, and Epstein MM (2019). Th2-T(RMs) Maintain Life-Long Allergic Memory in Experimental Asthma in Mice. Front Immunol 10, 840. 10.3389/fimmu.2019.00840. [PubMed: 31105692]

21. Lloyd CM, and Hessel EM (2010). Functions of T cells in asthma: more than just T(H)2 cells. Nat Rev Immunol 10, 838–848. 10.1038/nri2870. [PubMed: 21060320]

22. Seumois G, Ramírez-Suástegui C, Schmiedel BJ, Liang S, Peters B, Sette A, and Vijayanand P. (2020). Single-cell transcriptomic analysis of allergen-specific T cells in allergy and asthma. Science Immunology 5, eaba6087. 10.1126/sciimmunol.aba6087.

23. Alladina J, Smith NP, Kooistra T, Slowikowski K, Kernin IJ, Deguine J, Keen HL, Manakongtreecheep K, Tantivit J, Rahimi RA, et al. (2023). A human model of asthma exacerbation reveals transcriptional programs and cell circuits specific to allergic asthma. Science Immunology 8, eabq6352. doi:10.1126/sciimmunol.abq6352.

24. Rahimi RA, Nepal K, Cetinbas M, Sadreyev RI, and Luster AD (2020). Distinct functions of tissue-resident and circulating memory Th2 cells in allergic airway disease. J Exp Med 217. 10.1084/jem.20190865.

25. Ichikawa T, Hirahara K, Kokubo K, Kiuchi M, Aoki A, Morimoto Y, Kumagai J, Onodera A, Mato N, Tumes DJ, et al. (2019). CD103(hi) Treg cells constrain lung fibrosis induced by CD103(lo) tissue-resident pathogenic CD4 T cells. Nat Immunol 20, 1469–1480. 10.1038/s41590-019-0494-y. [PubMed: 31591568]

26. Turner DL, Goldklang M, Cvetkovski F, Paik D, Trischler J, Barahona J, Cao M, Dave R, Tanna N, D'Armiento JM, and Farber DL (2018). Biased Generation and In Situ Activation of Lung Tissue-Resident Memory CD4 T Cells in the Pathogenesis of Allergic Asthma. J Immunol 200, 1561–1569. 10.4049/jimmunol.1700257. [PubMed: 29343554]

27. Szabo PA, Miron M, and Farber DL (2019). Location, location, location: Tissue resident memory T cells in mice and humans. Sci Immunol 4. 10.1126/sciimmunol.aas9673.

28. Snyder ME, and Farber DL (2019). Human lung tissue resident memory T cells in health and disease. Current Opinion in Immunology 59, 101–108. 10.1016/j.coi.2019.05.011. [PubMed: 31265968]

29. Camiolo MJ, Zhou X, Oriss TB, Yan Q, Gorry M, Horne W, Trudeau JB, Scholl K, Chen W, Kolls JK, et al. (2021). High-dimensional profiling clusters asthma severity by lymphoid and non-lymphoid status. Cell Rep 35, 108974. 10.1016/j.celrep.2021.108974.

30. Hinks TS, Zhou X, Staples KJ, Dimitrov BD, Manta A, Petrossian T, Lum PY, Smith CG, Ward JA, Howarth PH, et al. (2015). Innate and adaptive T cells in asthmatic patients: Relationship to severity and disease mechanisms. J Allergy Clin Immunol 136, 323–333. 10.1016/j.jaci.2015.01.014. [PubMed: 25746968]

31. Muehling LM, Lawrence MG, and Woodfolk JA (2017). Pathogenic CD4(+) T cells in patients with asthma. J Allergy Clin Immunol 140, 1523–1540. 10.1016/j.jaci.2017.02.025. [PubMed: 28442213]

32. Seumois G, and Vijayanand P. (2019). Single-cell analysis to understand the diversity of immune cell types that drive disease pathogenesis. J Allergy Clin Immunol 144, 1150–1153. 10.1016/j.jaci.2019.09.014. [PubMed: 31703762]

33. Clarke J, Panwar B, Madrigal A, Singh D, Gujar R, Wood O, Chee SJ, Eschweiler S, King EV, Awad AS, et al. (2019). Single-cell transcriptomic analysis of tissue-resident memory T cells in human lung cancer. J Exp Med 216, 2128–2149. 10.1084/jem.20190249. [PubMed: 31227543]

34. Jaeger N, Gamini R, Cella M, Schettini JL, Bugatti M, Zhao S, Rosadini CV, Esaulova E, Di Luccia B, Kinnett B, et al. (2021). Single-cell analyses of Crohn's disease tissues reveal intestinal intraepithelial T cells heterogeneity and altered subset distributions. Nature Communications 12, 1921. 10.1038/s41467-021-22164-6.

35. Wu X, Liu Y, Jin S, Wang M, Jiao Y, Yang B, Lu X, Ji X, Fei Y, Yang H, et al. (2021). Single-cell sequencing of immune cells from anticitrullinated peptide antibody positive and negative rheumatoid arthritis. Nature Communications 12, 4977. 10.1038/s41467-021-25246-7.

36. Nehar-Belaid D, Hong S, Marches R, Chen G, Bolisetty M, Baisch J, Walters L, Punaro M, Rossi RJ, Chung C-H, et al. (2020). Mapping systemic lupus erythematosus heterogeneity at the single-cell level. Nature Immunology 21, 1094–1106. 10.1038/s41590-020-0743-0. [PubMed: 32747814]

37. Eschweiler S, Clarke J, Ramírez-Suástegui C, Panwar B, Madrigal A, Chee SJ, Karydis I, Woo E, Alzetani A, Elsheikh S, et al. (2021). Intratumoral follicular regulatory T cells curtail anti-PD-1 treatment efficacy. Nat Immunol 22, 1052–1063. 10.1038/s41590-021-00958-6. [PubMed: 34168370]

38. Eschweiler S, Ramírez-Suástegui C, Li Y, King E, Chudley L, Thomas J, Wood O, von Witzleben A, Jeffrey D, McCann K, et al. (2022). Intermittent PI3Kδ inhibition sustains anti-tumour immunity and curbs irAEs. Nature 605, 741–746. 10.1038/s41586-022-04685-2. [PubMed: 35508656]

39. Sikkema L, Ramírez-Suástegui C, Strobl DC, Gillett TE, Zappia L, Madissoon E, Markov NS, Zaragosi LE, Ji Y, Ansari M, et al. (2023). An integrated cell atlas of the lung in health and disease. Nat Med 29, 1563–1577. 10.1038/s41591-023-02327-2. [PubMed: 37291214]
40. Vieira Braga FA, Kar G, Berg M, Carpaij OA, Polanski K, Simon LM, Brouwer S, Gomes T, Hesse L, Jiang J, et al. (2019). A cellular census of human lungs identifies novel cell states in health and in asthma. Nat Med 25, 1153–1163. 10.1038/s41591-019-0468-5. [PubMed: 31209336]
41. Azim A, Mistry H, Freeman A, Barber C, Newell C, Gove K, Thirlwall Y, Harvey M, Bentley K, Knight D, et al. (2019). Protocol for the Wessex AsThma CoHort of difficult asthma (WATCH): a pragmatic real-life longitudinal study of difficult asthma in the clinic. BMC Pulm Med 19, 99. 10.1186/s12890-019-0862-2. [PubMed: 31126281]
42. Larsson K, Kankaanranta H, Janson C, Lehtimäki L, Ställberg B, Løkke A, Høines K, Roslind K, and Ulrik CS (2020). Bringing asthma care into the twenty-first century. npj Primary Care Respiratory Medicine 30, 25. 10.1038/s41533-020-0182-2.
43. Global Initiative for Asthma. Global Strategy for Asthma Management and Prevention, 2021. www.ginasthma.org.
44. Diniz MO, Mitsi E, Swadling L, Rylance J, Johnson M, Goldblatt D, Ferreira D, and Maini MK (2022). Airway-resident T cells from unexposed individuals cross-recognize SARS-CoV-2. Nature Immunology 23, 1324–1329. 10.1038/s41590-022-01292-1. [PubMed: 36038709]
45. Tang J, Zeng C, Cox TM, Li C, Son YM, Cheon IS, Wu Y, Behl S, Taylor JJ, Chakaraborty R, et al. (2022). Respiratory mucosal immunity against SARS-CoV-2 after mRNA vaccination. Science Immunology 7, eadd4853. doi:10.1126/sciimmunol.add4853.
46. Liao M, Liu Y, Yuan J, Wen Y, Xu G, Zhao J, Cheng L, Li J, Wang X, Wang F, et al. (2020). Single-cell landscape of bronchoalveolar immune cells in patients with COVID-19. Nature Medicine 26, 842–844. 10.1038/s41591-020-0901-9.
47. Grant RA, Morales-Nebreda L, Markov NS, Swaminathan S, Querrey M, Guzman ER, Abbott DA, Donnelly HK, Donayre A, Goldberg IA, et al. (2021). Circuits between infected macrophages and T cells in SARS-CoV-2 pneumonia. Nature 590, 635–641. 10.1038/s41586-020-03148-w. [PubMed: 33429418]
48. Morse C, Tabib T, Sembrat J, Buschur KL, Bittar HT, Valenzi E, Jiang Y, Kass DJ, Gibson K, Chen W, et al. (2019). Proliferating SPP1/MERTK-expressing macrophages in idiopathic pulmonary fibrosis. Eur Respir J 54. 10.1183/13993003.02441-2018.
49. Mould KJ, Moore CM, McManus SA, McCubbrey AL, McClendon JD, Griesmer CL, Henson PM, and Janssen WJ (2021). Airspace Macrophages and Monocytes Exist in Transcriptionally Distinct Subsets in Healthy Adults. Am J Respir Crit Care Med 203, 946–956. 10.1164/rccm.202005l989OC. [PubMed: 33079572]
50. Oja AE, Piet B, Helbig C, Stark R, van der Zwan D, Blaauwgeers H, Remmerswaal EBM, Amsen D, Jonkers RE, Moerland PD, et al. (2018). Trigger-happy resident memory CD4+ T cells inhabit the human lungs. Mucosal Immunology 11, 654–667. 10.1038/mi.2017.94. [PubMed: 29139478]
51. Kumar BV, Ma W, Miron M, Granot T, Guyer RS, Carpenter DJ, Senda T, Sun X, Ho SH, Lerner H, et al. (2017). Human Tissue-Resident Memory T Cells Are Defined by Core Transcriptional and Functional Signatures in Lymphoid and Mucosal Sites. Cell Rep 20, 2921–2934. 10.1016/j.celrep.2017.08.078. [PubMed: 28930685]
52. Casey KA, Fraser KA, Schenkel JM, Moran A, Abt MC, Beura LK, Lucas PJ, Artis D, Wherry EJ, Hogquist K, et al. (2012). Antigen-independent differentiation and maintenance of effector-like resident memory T cells in tissues. J Immunol 188, 4866–4875. 10.4049/jimmunol.1200402. [PubMed: 22504644]
53. Cepek KL, Shaw SK, Parker CM, Russell GJ, Morrow JS, Rimm DL, and Brenner MB (1994). Adhesion between epithelial cells and T lymphocytes mediated by E-cadherin and the alpha E beta 7 integrin. Nature 372, 190–193. 10.1038/372190a0. [PubMed: 7969453]
54. Arnon TI, Xu Y, Lo C, Pham T, An J, Coughlin S, Dorn GW, and Cyster JG (2011). GRK2-dependent S1PR1 desensitization is required for lymphocytes to overcome their attraction to blood. Science 333, 1898–1903. 10.1126/science.1208248. [PubMed: 21960637]

55. Porter JC, and Hall A. (2009). Epithelial ICAM-1 and ICAM-2 regulate the egression of human T cells across the bronchial epithelium. Faseb j 23, 492–502. 10.1096/fj.08-115899. [PubMed: 18842965]

56. Petiti L, and Pace L. (2020). The persistence of stemness. Nature Immunology 21, 492–494. 10.1038/s41590-020-0644-2. [PubMed: 32231299]

57. Rudensky AY (2011). Regulatory T cells and Foxp3. Immunol Rev 241, 260–268. 10.1111/j.1600-065X.2011.01018.x. [PubMed: 21488902]

58. Schmiedel BJ, Singh D, Madrigal A, Valdovino-Gonzalez AG, White BM, Zapardiel-Gonzalo J, Ha B, Altay G, Greenbaum JA, McVicker G, et al. (2018). Impact of Genetic Polymorphisms on Human Immune Cell Gene Expression. Cell 175, 1701–1715.e1716. 10.1016/j.cell.2018.10.022. [PubMed: 30449622]

59. Locci M, Havenar-Daughton C, Landais E, Wu J, Kroenke MA, Arlehamn CL, Su LF, Cubas R, Davis MM, Sette A, et al. (2013). Human circulating PD-1+CXCR3-CXCR5+ memory Tfh cells are highly functional and correlate with broadly neutralizing HIV antibody responses. Immunity 39, 758–769. 10.1016/j.immuni.2013.08.031. [PubMed: 24035365]

60. Best JA, Blair DA, Knell J, Yang E, Mayya V, Doedens A, Dustin ML, and Goldrath AW (2013). Transcriptional insights into the CD8(+) T cell response to infection and memory T cell formation. Nat Immunol 14, 404–412. 10.1038/ni.2536. [PubMed: 23396170]

61. Patil VS, Madrigal A, Schmiedel BJ, Clarke J, O'Rourke P, de Silva AD, Harris E, Peters B, Seumois G, Weiskopf D, et al. (2018). Precursors of human $CD4^{+}$ cytotoxic T lymphocytes identified by single-cell transcriptome analysis. Science Immunology 3, eaan8664. 10.1126/sciimmunol.aan8664.

62. Azim A, Freeman A, Lavenu A, Mistry H, Haitchi HM, Newell C, Cheng Y, Thirlwall Y, Harvey M, Barber C, et al. (2020). New Perspectives on Difficult Asthma; Sex and Age of Asthma-Onset Based Phenotypes. The Journal of Allergy and Clinical Immunology: In Practice 8, 3396–3406.e3394. 10.1016/j.jaip.2020.05.053. [PubMed: 32544545]

63. Amelink M, de Nijs SB, Berger M, Weersink EJ, ten Brinke A, Sterk PJ, and Bel EH (2012). Non-atopic males with adult onset asthma are at risk of persistent airflow limitation. Clin Exp Allergy 42, 769–774. 10.1111/j.1365-2222.2012.03977.x. [PubMed: 22515392]

64. Fitzpatrick AM, Szefler SJ, Mauger DT, Phillips BR, Denlinger LC, Moore WC, Sorkness RL, Wenzel SE, Gergen PJ, Bleecker ER, et al. (2020). Development and initial validation of the Asthma Severity Scoring System (ASSESS). J Allergy Clin Immunol 145, 127–139. 10.1016/j.jaci.2019.09.018. [PubMed: 31604088]

65. Teague WG, Phillips BR, Fahy JV, Wenzel SE, Fitzpatrick AM, Moore WC, Hastie AT, Bleecker ER, Meyers DA, Peters SP, et al. (2018). Baseline Features of the Severe Asthma Research Program (SARP III) Cohort: Differences with Age. J Allergy Clin Immunol Pract 6, 545–554.e544. 10.1016/j.jaip.2017.05.032. [PubMed: 28866107]

66. Grychtol R, Riemann L, Gaedcke S, Liu B, DeLuca D, Förster R, Maison N, Thiele D, Jakobs N, Bahmer T, et al. (2023). Validation of the Asthma Severity Scoring System (ASSESS) in the ALLIANCE cohort. J Allergy Clin Immunol. 10.1016/j.jaci.2023.01.027.

67. Tippalagama R, Singhania A, Dubelko P, Lindestam Arlehamn CS, Crinklaw A, Pomaznoy M, Seumois G, deSilva AD, Premawansa S, Vidanagama D, et al. (2021). HLA-DR Marks Recently Divided Antigen-Specific Effector CD4 T Cells in Active Tuberculosis Patients. J Immunol. 10.4049/jimmunol.2100011.

68. Berbers RM, van der Wal MM, van Montfrans JM, Ellerbroek PM, Dalm V, van Hagen PM, Leavis HL, and van Wijk F. (2021). Chronically Activated T-cells Retain Their Inflammatory Properties in Common Variable Immunodeficiency. J Clin Immunol. 10.1007/s10875-021-01084-6.

69. Makris S, Paulsen M, and Johansson C. (2017). Type I Interferons as Regulators of Lung Inflammation. Front Immunol 8, 259. 10.3389/fimmu.2017.00259. [PubMed: 28344581]

70. Choi IW, Sun K, Kim YS, Ko HM, Im SY, Kim JH, You HJ, Lee YC, Lee JH, Park YM, and Lee HK (2005). TNF-alpha induces the late-phase airway hyperresponsiveness and airway inflammation through cytosolic phospholipase A(2) activation. J Allergy Clin Immunol 116, 537–543. 10.1016/j.jaci.2005.05.034. [PubMed: 16159621]

71. Doherty TA, Soroosh P, Khorram N, Fukuyama S, Rosenthal P, Cho JY, Norris PS, Choi H, Scheu S, Pfeffer K, et al. (2011). The tumor necrosis factor family member LIGHT is a target for asthmatic airway remodeling. Nat Med 17, 596–603. 10.1038/nm.2356. [PubMed: 21499267]
72. Mackay LK, Minnich M, Kragten NA, Liao Y, Nota B, Seillet C, Zaid A, Man K, Preston S, Freestone D, et al. (2016). Hobit and Blimp1 instruct a universal transcriptional program of tissue residency in lymphocytes. Science 352, 459–463. 10.1126/science.aad2035. [PubMed: 27102484]
73. Oja AE, Vieira Braga FA, Remmerswaal EB, Kragten NA, Hertoghs KM, Zuo J, Moss PA, van Lier RA, van Gisbergen KP, and Hombrink P. (2017). The Transcription Factor Hobit Identifies Human Cytotoxic CD4(+) T Cells. Front Immunol 8, 325. 10.3389/fimmu.2017.00325. [PubMed: 28392788]
74. Serroukh Y, Gu-Trantien C, Hooshiar Kashani B, Defrance M, Vu Manh TP, Azouz A, Detavernier A, Hoyois A, Das J, Bizet M, et al. (2018). The transcription factors Runx3 and ThPOK cross-regulate acquisition of cytotoxic function by human Th1 lymphocytes. Elife 7. 10.7554/eLife.30496.
75. Omilusik KD, Best JA, Yu B, Goossens S, Weidemann A, Nguyen JV, Seuntjens E, Stryjewska A, Zweier C, Roychoudhuri R, et al. (2015). Transcriptional repressor ZEB2 promotes terminal differentiation of CD8+ effector and memory T cell populations during infection. J Exp Med 212, 2027–2039. 10.1084/jem.20150194. [PubMed: 26503445]
76. Albrecht I, Niesner U, Janke M, Menning A, Loddenkemper C, Kühl AA, Lepenies I, Lexberg MH, Westendorf K, Hradilkova K, et al. (2010). Persistence of effector memory Th1 cells is regulated by Hopx. Eur J Immunol 40, 2993–3006. 10.1002/eji.201040936. [PubMed: 21061432]
77. Lang R, and Raffi FAM (2019). Dual-Specificity Phosphatases in Immunity and Infection: An Update. Int J Mol Sci 20. 10.3390/ijms20112710.
78. Lang R, Hammer M, and Mages J. (2006). DUSP meet immunology: dual specificity MAPK phosphatases in control of the inflammatory response. J Immunol 177, 7497–7504. 10.4049/jimmunol.177.11.7497. [PubMed: 17114416]
79. Verjans E, Ohl K, Reiss LK, van Wijk F, Toncheva AA, Wiener A, Yu Y, Rieg AD, Gaertner VD, Roth J, et al. (2015). The cAMP response element modulator (CREM) regulates TH2 mediated inflammation. Oncotarget 6, 38538–38551. 10.18632/oncotarget.6041. [PubMed: 26459392]
80. Koga T, Hedrich CM, Mizui M, Yoshida N, Otomo K, Lieberman LA, Rauen T, Crispín JC, and Tsokos GC (2014). CaMK4-dependent activation of AKT/mTOR and CREM-α underlies autoimmunity-associated Th17 imbalance. J Clin Invest 124, 2234–2245. 10.1172/jci73411. [PubMed: 24667640]
81. Giordano M, Roncagalli R, Bourdely P, Chasson L, Buferne M, Yamasaki S, Beyaert R, van Loo G, Auphan-Anezin N, Schmitt-Verhulst A-M, and Verdeil G. (2014). The tumor necrosis factor alpha-induced protein 3 (TNFAIP3, A20) imposes a brake on antitumor activity of CD8 T cells. Proceedings of the National Academy of Sciences 111, 11115–11120. 10.1073/pnas.1406259111.
82. Shah S, King EM, Chandrasekhar A, and Newton R. (2014). Roles for the mitogen-activated protein kinase (MAPK) phosphatase, DUSP1, in feedback control of inflammatory gene expression and repression by dexamethasone. J Biol Chem 289, 13667–13679. 10.1074/jbc.M113.540799. [PubMed: 24692548]
83. Hoppstädter J, and Ammit AJ (2019). Role of Dual-Specificity Phosphatase 1 in Glucocorticoid-Driven Anti-inflammatory Responses. Frontiers in Immunology 10. 10.3389/fimmu.2019.01446.
84. Sun F, Yue T-T, Yang C-L, Wang F-X, Luo J-H, Rong S-J, Zhang M, Guo Y, Xiong F, and Wang C-Y (2021). The MAPK dual specific phosphatase (DUSP) proteins: A versatile wrestler in T cell functionality. International Immunopharmacology 98, 107906. 10.1016/j.intimp.2021.107906.
85. Lu D, Liu L, Ji X, Gao Y, Chen X, Liu Y, Liu Y, Zhao X, Li Y, Li Y, et al. (2015). The phosphatase DUSP2 controls the activity of the transcription activator STAT3 and regulates TH17 differentiation. Nature Immunology 16, 1263–1273. 10.1038/ni.3278. [PubMed: 26479789]
86. Hsiao WY, Lin YC, Liao FH, Chan YC, and Huang CY (2015). Dual-Specificity Phosphatase 4 Regulates STAT5 Protein Stability and Helper T Cell Polarization. PLoS One 10, e0145880. 10.1371/journal.pone.0145880.

87. Sakakibara S, Espigol-Frigole G, Gasperini P, Uldrick TS, Yarchoan R, and Tosato G. (2013). A20/TNFAIP3 inhibits NF-κB activation induced by the Kaposi's sarcoma-associated herpesvirus vFLIP oncoprotein. Oncogene 32, 1223–1232. 10.1038/onc.2012.145. [PubMed: 22525270]

88. Harhaj EW, and Dixit VM (2012). Regulation of NF-κB by deubiquitinases. Immunol Rev 246, 107–124. 10.1111/j.1600-065X.2012.01100.x. [PubMed: 22435550]

89. Weathington N, O'Brien ME, Radder J, Whisenant TC, Bleecker ER, Busse WW, Erzurum SC, Gaston B, Hastie AT, Jarjour NN, et al. (2019). BAL Cell Gene Expression in Severe Asthma Reveals Mechanisms of Severe Disease and Influences of Medications. Am J Respir Crit Care Med 200, 837–856. 10.1164/rccm.201811-2221OC. [PubMed: 31161938]

90. Li H, Su P, Lai TKY, Jiang A, Liu J, Zhai D, Campbell CTG, Lee FHF, Yong W, Pasricha S, et al. (2020). The glucocorticoid receptor–FKBP51 complex contributes to fear conditioning and posttraumatic stress disorder. The Journal of Clinical Investigation 130, 877–889. 10.1172/JCI130363. [PubMed: 31929189]

91. Sharma S, Kho AT, Chhabra D, Qiu W, Gaedigk R, Vyhlidal CA, Leeder JS, Barraza-Villarreal A, London SJ, Gilliland F, et al. (2015). Glucocorticoid genes and the developmental origins of asthma susceptibility and treatment response. Am J Respir Cell Mol Biol 52, 543–553. 10.1165/rcmb.2014-0109OC. [PubMed: 25192440]

92. Galigniana NM, Ballmer LT, Toneatto J, Erlejman AG, Lagadari M, and Galigniana MD (2012). Regulation of the glucocorticoid response to stress-related disorders by the Hsp90-binding immunophilin FKBP51. Journal of Neurochemistry 122, 4–18. 10.1111/j.1471-4159.2012.07775.x. [PubMed: 22548329]

93. Anderson AC, Joller N, and Kuchroo VK (2016). Lag-3, Tim-3, and TIGIT: Co-inhibitory Receptors with Specialized Functions in Immune Regulation. Immunity 44, 989–1004. 10.1016/j.immuni.2016.05.001. [PubMed: 27192565]

94. Lee SM, Gao B, and Fang D. (2008). FoxP3 maintains Treg unresponsiveness by selectively inhibiting the promoter DNA-binding activity of AP-1. Blood 111, 3599–3606. 10.1182/blood-2007-09-115014. [PubMed: 18223166]

95. Koizumi S. i., Sasaki D, Hsieh T-H, Taira N, Arakaki N, Yamasaki S, Wang K, Sarkar S, Shirahata H, Miyagi M, and Ishikawa H. (2018). JunB regulates homeostasis and suppressive functions of effector regulatory T cells. Nature Communications 9, 5344. 10.1038/s41467-018-07735-4.

96. Meckiff BJ, Ramírez-Suástegui C, Fajardo V, Chee SJ, Kusnadi A, Simon H, Eschweiler S, Grifoni A, Pelosi E, Weiskopf D, et al. (2020). Imbalance of Regulatory and Cytotoxic SARS-CoV2-Reactive CD4(+) T Cells in COVID-19. Cell 183, 1340–1353.e1316. 10.1016/j.cell.2020.10.001. [PubMed: 33096020]

97. Wang Y, Chen Z, Wang T, Guo H, Liu Y, Dang N, Hu S, Wu L, Zhang C, Ye K, and Shi B. (2021). A novel CD4+ CTL subtype characterized by chemotaxis and inflammation is involved in the pathogenesis of Graves' orbitopathy. Cellular & Molecular Immunology 18, 735–745. 10.1038/s41423-020-00615-2. [PubMed: 33514849]

98. Juno JA, van Bockel D, Kent SJ, Kelleher AD, Zaunders JJ, and Munier CM (2017). Cytotoxic CD4 T Cells-Friend or Foe during Viral Infection? Front Immunol 8, 19. 10.3389/fimmu.2017.00019. [PubMed: 28167943]

99. Hughes CE, and Nibbs RJB (2018). A guide to chemokines and their receptors. FEBS J 285, 2944–2971. 10.1111/febs.14466. [PubMed: 29637711]

100. Maehara T, Kaneko N, Perugino CA, Mattoo H, Kers J, Allard-Chamard H, Mahajan VS, Liu H, Murphy SJ, Ghebremichael M, et al. (2020). Cytotoxic CD4+ T lymphocytes may induce endothelial cell apoptosis in systemic sclerosis. J Clin Invest 130, 2451–2464. 10.1172/jci131700. [PubMed: 31990684]

101. Mattoo H, Mahajan VS, Maehara T, Deshpande V, Della-Torre E, Wallace ZS, Kulikova M, Drijvers JM, Daccache J, Carruthers MN, et al. (2016). Clonal expansion of CD4(+) cytotoxic T lymphocytes in patients with IgG4-related disease. J Allergy Clin Immunol 138, 825–838. 10.1016/j.jaci.2015.12.1330. [PubMed: 26971690]

102. Lundblad LK, Thompson-Figueroa J, Leclair T, Sullivan MJ, Poynter ME, Irvin CG, and Bates JH (2005). Tumor necrosis factor-alpha overexpression in lung disease: a single cause behind a complex phenotype. Am J Respir Crit Care Med 171, 1363–1370. 10.1164/rccm.200410-1349OC. [PubMed: 15805183]

103. Mukhopadhyay S, Hoidal JR, and Mukherjee TK (2006). Role of TNFα in pulmonary pathophysiology. Respiratory Research 7, 125. 10.1186/1465-9921-7-125. [PubMed: 17034639]
104. Becher B, Tugues S, and Greter M. (2016). GM-CSF: From Growth Factor to Central Mediator of Tissue Inflammation. Immunity 45, 963–973. 10.1016/j.immuni.2016.10.026. [PubMed: 27851925]
105. Zhao J, Lloyd CM, and Noble A. (2013). Th17 responses in chronic allergic airway inflammation abrogate regulatory T-cell-mediated tolerance and contribute to airway remodeling. Mucosal Immunology 6, 335–346. 10.1038/mi.2012.76. [PubMed: 22892938]
106. Newcomb DC, and Peebles RS Jr. (2013). Th17-mediated inflammation in asthma. Curr Opin Immunol 25, 755–760. 10.1016/j.coi.2013.08.002. [PubMed: 24035139]
107. Lee HS, Park D-E, Lee J-W, Sohn KH, Cho S-H, and Park H-W (2020). Role of interleukin-23 in the development of nonallergic eosinophilic inflammation in a murine model of asthma. Experimental & Molecular Medicine 52, 92–104. 10.1038/s12276-019-0361-9. [PubMed: 31956268]
108. Tortola L, Pawelski H, Sonar SS, Ampenberger F, Kurrer M, and Kopf M. (2019). IL-21 promotes allergic airway inflammation by driving apoptosis of FoxP3(+) regulatory T cells. J Allergy Clin Immunol 143, 2178–2189.e2175. 10.1016/j.jaci.2018.11.047. [PubMed: 30654048]
109. da Silva Antunes R, Mehta AK, Madge L, Tocker J, and Croft M. (2018). TNFSF14 (LIGHT) Exhibits Inflammatory Activities in Lung Fibroblasts Complementary to IL-13 and TGF-β. Frontiers in Immunology 9. 10.3389/fimmu.2018.00576.
110. Qiu HN, Wong CK, Dong J, Lam CW, and Cai Z. (2014). Effect of tumor necrosis factor family member LIGHT (TNFSF14) on the activation of basophils and eosinophils interacting with bronchial epithelial cells. Mediators Inflamm 2014, 136463. 10.1155/2014/136463.
111. Coquet JM, Schuijs MJ, Smyth MJ, Deswarte K, Beyaert R, Braun H, Boon L, Karlsson Hedestam GB, Nutt SL, Hammad H, and Lambrecht BN (2015). Interleukin-21-Producing CD4(+) T Cells Promote Type 2 Immunity to House Dust Mites. Immunity 43, 318–330. 10.1016/j.immuni.2015.07.015. [PubMed: 26287681]
112. Kuruvilla ME, Lee FE, and Lee GB (2019). Understanding Asthma Phenotypes, Endotypes, and Mechanisms of Disease. Clin Rev Allergy Immunol 56, 219–233. 10.1007/s12016-018-8712-1. [PubMed: 30206782]
113. Ray A, Das J, and Wenzel SE (2022). Determining asthma endotypes and outcomes: Complementing existing clinical practice with modern machine learning. Cell Rep Med 3, 100857. 10.1016/j.xcrm.2022.100857.
114. Haldar P, Pavord ID, Shaw DE, Berry MA, Thomas M, Brightling CE, Wardlaw AJ, and Green RH (2008). Cluster analysis and clinical asthma phenotypes. Am J Respir Crit Care Med 178, 218–224. 10.1164/rccm.200711-1754OC. [PubMed: 18480428]
115. Siroux V, Basagaña X, Boudier A, Pin I, Garcia-Aymerich J, Vesin A, Slama R, Jarvis D, Anto JM, Kauffmann F, and Sunyer J. (2011). Identifying adult asthma phenotypes using a clustering approach. European Respiratory Journal 38, 310–317. 10.1183/09031936.00120810. [PubMed: 21233270]
116. Newby C, Heaney LG, Menzies-Gow A, Niven RM, Mansur A, Bucknall C, Chaudhuri R, Thompson J, Burton P, and Brightling C. (2014). Statistical cluster analysis of the British Thoracic Society Severe refractory Asthma Registry: clinical outcomes and phenotype stability. PLoS One 9, e102987. 10.1371/journal.pone.0102987. [PubMed: 25058007]
117. Ilmarinen P, Tuomisto LE, Niemelä O, Tommola M, Haanpää J, and Kankaanranta H. (2017). Cluster Analysis on Longitudinal Data of Patients with Adult-Onset Asthma. J Allergy Clin Immunol Pract 5, 967–978.e963. 10.1016/j.jaip.2017.01.027. [PubMed: 28389304]
118. Liu S, Liu C, Wang Q, Liu S, and Min J. (2023). CC Chemokines in Idiopathic Pulmonary Fibrosis: Pathogenic Role and Therapeutic Potential. Biomolecules 13. 10.3390/biom13020333.
119. Zhou Z, He H, Wang K, Shi X, Wang Y, Su Y, Wang Y, Li D, Liu W, Zhang Y, et al. (2020). Granzyme A from cytotoxic lymphocytes cleaves GSDMB to trigger pyroptosis in target cells. Science 368. 10.1126/science.aaz7548.
120. Cheroutre H, and Husain MM (2013). CD4 CTL: living up to the challenge. Semin Immunol 25, 273–281. 10.1016/j.smim.2013.10.022. [PubMed: 24246226]

121. Weiskopf D, Bangs DJ, Sidney J, Kolla RV, De Silva AD, de Silva AM, Crotty S, Peters B, and Sette A. (2015). Dengue virus infection elicits highly polarized CX3CR1+ cytotoxic CD4+ T cells associated with protective immunity. Proc Natl Acad Sci U S A 112, E4256–4263. 10.1073/pnas.1505956112. [PubMed: 26195744]

122. Derhovanessian E, Maier AB, Hahnel K, Beck R, de Craen AJ, Slagboom EP, Westendorp RG, and Pawelec G. (2011). Infection with cytomegalovirus but not herpes simplex virus induces the accumulation of late-differentiated CD4+ and CD8+ T-cells in humans. J Gen Virol 92, 2746–2756. 10.1099/vir.0.036004-0. [PubMed: 21813708]

123. Intlekofer AM, Takemoto N, Wherry EJ, Longworth SA, Northrup JT, Palanivel VR, Mullen AC, Gasink CR, Kaech SM, Miller JD, et al. (2005). Effector and memory CD8+ T cell fate coupled by T-bet and eomesodermin. Nature immunology 6, 1236–1244. 10.1038/ni1268. [PubMed: 16273099]

124. Takemoto N, Intlekofer AM, Northrup JT, Wherry EJ, and Reiner SL (2006). Cutting Edge: IL-12 inversely regulates T-bet and eomesodermin expression during pathogen-induced CD8+ T cell differentiation. Journal of immunology 177, 7515–7519.

125. Appay V, Zaunders JJ, Papagno L, Sutton J, Jaramillo A, Waters A, Easterbrook P, Grey P, Smith D, McMichael AJ, et al. (2002). Characterization of CD4(+) CTLs ex vivo. Journal of immunology 168, 5954–5958.

126. Zaunders JJ, Dyer WB, Wang B, Munier ML, Miranda-Saksena M, Newton R, Moore J, Mackay CR, Cooper DA, Saksena NK, and Kelleher AD (2004). Identification of circulating antigen-specific CD4+ T lymphocytes with a CCR5+, cytotoxic phenotype in an HIV-1 long-term nonprogressor and in CMV infection. Blood 103, 2238–2247. 10.1182/blood-2003-08-2765. [PubMed: 14645006]

127. Norris PJ, Moffett HF, Yang OO, Kaufmann DE, Clark MJ, Addo MM, and Rosenberg ES (2004). Beyond help: direct effector functions of human immunodeficiency virus type 1-specific CD4(+) T cells. Journal of virology 78, 8844–8851. 10.1128/JVI.78.16.8844-8851.2004. [PubMed: 15280492]

128. van Leeuwen EM, Remmerswaal EB, Vossen MT, Rowshani AT, Wertheim-van Dillen PM, van Lier RA, and ten Berge IJ (2004). Emergence of a CD4+CD28-granzyme B+, cytomegalovirus-specific T cell subset after recovery of primary cytomegalovirus infection. Journal of immunology 173, 1834–1841.

129. Aslan N, Yurdaydin C, Wiegand J, Greten T, Ciner A, Meyer MF, Heiken H, Kuhlmann B, Kaiser T, Bozkaya H, et al. (2006). Cytotoxic CD4 T cells in viral hepatitis. J Viral Hepat 13, 505–514. 10.1111/j.1365-2893.2006.00723.x. [PubMed: 16901280]

130. Wilkinson TM, Li CK, Chui CS, Huang AK, Perkins M, Liebner JC, Lambkin-Williams R, Gilbert A, Oxford J, Nicholas B, et al. (2012). Preexisting influenza-specific CD4+ T cells correlate with disease protection against influenza challenge in humans. Nat Med 18, 274–280. 10.1038/nm.2612. [PubMed: 22286307]

131. Fonseka CY, Rao DA, Teslovich NC, Korsunsky I, Hannes SK, Slowikowski K, Gurish MF, Donlin LT, Lederer JA, Weinblatt ME, et al. (2018). Mixed-effects association of single cells identifies an expanded effector CD4(+) T cell subset in rheumatoid arthritis. Science translational medicine 10. 10.1126/scitranslmed.aaq0305.

132. Schafflick D, Xu CA, Hartlehnert M, Cole M, Schulte-Mecklenbeck A, Lautwein T, Wolbert J, Heming M, Meuth SG, Kuhlmann T, et al. (2020). Integrated single cell analysis of blood and cerebrospinal fluid leukocytes in multiple sclerosis. Nature communications 11, 247. 10.1038/s41467-019-14118-w.

133. Gilani SR, Vuga LJ, Lindell KO, Gibson KF, Xue J, Kaminski N, Valentine VG, Lindsay EK, George MP, Steele C, and Duncan SR (2010). CD28 down-regulation on circulating CD4 T-cells is associated with poor prognoses of patients with idiopathic pulmonary fibrosis. PLoS One 5, e8959. 10.1371/journal.pone.0008959. [PubMed: 20126467]

134. Kim D, Park G, Huuhtanen J, Lundgren S, Khajuria RK, Hurtado AM, Munoz-Calleja C, Cardenoso L, Gomez-Garcia de Soria V, Chen-Liang TH, et al. (2020). Somatic mTOR mutation in clonally expanded T lymphocytes associated with chronic graft versus host disease. Nature communications 11, 2246. 10.1038/s41467-020-16115-w.

135. Mucida D, Husain MM, Muroi S, van Wijk F, Shinnakasu R, Naoe Y, Reis BS, Huang Y, Lambolez F, Docherty M, et al. (2013). Transcriptional reprogramming of mature CD4[+] helper T cells generates distinct MHC class II-restricted cytotoxic T lymphocytes. Nat Immunol 14, 281–289. 10.1038/ni.2523. [PubMed: 23334788]

136. Allard B, Levardon H, Esteves P, Celle A, Maurat E, Thumerel M, Girodet PO, Trian T, and Berger P. (2019). Asthmatic Bronchial Smooth Muscle Increases CCL5-Dependent Monocyte Migration in Response to Rhinovirus-Infected Epithelium. Front Immunol 10, 2998. 10.3389/fimmu.2019.02998. [PubMed: 31969885]

137. Jackson DJ, and Johnston SL (2010). The role of viruses in acute exacerbations of asthma. J Allergy Clin Immunol 125, 1178–1187; quiz 1188–1179. 10.1016/j.jaci.2010.04.021. [PubMed: 20513517]

138. Gauthier M, Kale SL, Oriss TB, Scholl K, Das S, Yuan H, Hu S, Chen J, Camiolo M, Ray P, et al. (2022). Dual role for CXCR3 and CCR5 in asthmatic type 1 inflammation. J Allergy Clin Immunol 149, 113–124.e117. 10.1016/j.jaci.2021.05.044. [PubMed: 34146578]

139. Gauthier M, Kale SL, Oriss TB, Gorry M, Ramonell RP, Dalton K, Ray P, Fahy JV, Seibold MA, Castro M, et al. (2023). CCL5 is a potential bridge between type 1 and type 2 inflammation in asthma. Journal of Allergy and Clinical Immunology 152, 94–106.e112. 10.1016/j.jaci.2023.02.028. [PubMed: 36893862]

140. Agusti A, Fabbri LM, Singh D, Vestbo J, Celli B, Franssen FM, Rabe KF, and Papi A. (2018). Inhaled corticosteroids in COPD: Friend or foe? European Respiratory Journal, 1801219. 10.1183/13993003.01219-2018.

141. Jenkins CR, Boulet LP, Lavoie KL, Raherison-Semjen C, and Singh D. (2022). Personalized Treatment of Asthma: The Importance of Sex and Gender Differences. J Allergy Clin Immunol Pract 10, 963–971.e963. 10.1016/j.jaip.2022.02.002. [PubMed: 35150902]

142. Yung JA, Fuseini H, and Newcomb DC (2018). Hormones, sex, and asthma. Ann Allergy Asthma Immunol 120, 488–494. 10.1016/j.anai.2018.01.016. [PubMed: 29410216]

143. Arshad SH, Holloway JW, Karmaus W, Zhang H, Ewart S, Mansfield L, Matthews S, Hodgekiss C, Roberts G, and Kurukulaaratchy R. (2018). Cohort Profile: The Isle Of Wight Whole Population Birth Cohort (IOWBC). Int J Epidemiol 47, 1043–1044i. 10.1093/ije/dyy023. [PubMed: 29547889]

144. Picelli S, Björklund ÅK, Faridani OR, Sagasser S, Winberg G, and Sandberg R. (2013). Smart-seq2 for sensitive full-length transcriptome profiling in single cells. Nature Methods 10, 1096–1098. 10.1038/nmeth.2639. [PubMed: 24056875]

145. Engel I, Seumois G, Chavez L, Samaniego-Castruita D, White B, Chawla A, Mock D, Vijayanand P, and Kronenberg M. (2016). Innate-like functions of natural killer T cell subsets result from highly divergent gene programs. Nat Immunol 17, 728–739. 10.1038/ni.3437. [PubMed: 27089380]

146. Rosales SL, Liang S, Engel I, Schmiedel BJ, Kronenberg M, Vijayanand P, and Seumois G. (2018). A Sensitive and Integrated Approach to Profile Messenger RNA from Samples with Low Cell Numbers. Methods Mol Biol 1799, 275–302. 10.1007/978-1-4939-7896-0_21. [PubMed: 29956159]

147. Love MI, Huber W, and Anders S. (2014). Moderated estimation of fold change and dispersion for RNA-seq data with DESeq2. Genome Biol 15, 550. 10.1186/s13059-014-0550-8. [PubMed: 25516281]

148. Bolotin DA, Poslavsky S, Mitrophanov I, Shugay M, Mamedov IZ, Putintseva EV, and Chudakov DM (2015). MiXCR: software for comprehensive adaptive immunity profiling. Nature Methods 12, 380–381. 10.1038/nmeth.3364. [PubMed: 25924071]

149. Shugay M, Bagaev DV, Turchaninova MA, Bolotin DA, Britanova OV, Putintseva EV, Pogorelyy MV, Nazarov VI, Zvyagin IV, Kirgizova VI, et al. (2015). VDJtools: Unifying Post-analysis of T Cell Receptor Repertoires. PLoS Comput Biol 11, e1004503. 10.1371/journal.pcbi.1004503.

150. 10x Genomics Cell Ranger 3.1.0.

151. Kang HM, Subramaniam M, Targ S, Nguyen M, Maliskova L, McCarthy E, Wan E, Wong S, Byrnes L, Lanata CM, et al. (2018). Multiplexed droplet single-cell RNA-sequencing using natural genetic variation. Nat Biotechnol 36, 89–94. 10.1038/nbt.4042. [PubMed: 29227470]

152. Stuart T, Butler A, Hoffman P, Hafemeister C, Papalexi E, Mauck WM 3rd, Hao Y, Stoeckius M, Smibert P, and Satija R. (2019). Comprehensive Integration of Single-Cell Data. Cell 177, 1888–1902.e1821. 10.1016/j.cell.2019.05.031. [PubMed: 31178118]

153. Korotkevich G, Sukhov V, Budin N, Shpak B, Artyomov MN, and Sergushichev A. (2021). Fast gene set enrichment analysis. bioRxiv, 060012. 10.1101/060012.

154. Hänzelmann S, Castelo R, and Guinney J. (2013). GSVA: gene set variation analysis for microarray and RNA-Seq data. BMC Bioinformatics 14, 7. 10.1186/1471-2105-14-7. [PubMed: 23323831]

155. Wu T, Hu E, Xu S, Chen M, Guo P, Dai Z, Feng T, Zhou L, Tang W, Zhan L, et al. (2021). clusterProfiler 4.0: A universal enrichment tool for interpreting omics data. Innovation (Camb) 2, 100141. 10.1016/j.xinn.2021.100141.

156. Finak G, McDavid A, Yajima M, Deng J, Gersuk V, Shalek AK, Slichter CK, Miller HW, McElrath MJ, Prlic M, et al. (2015). MAST: a flexible statistical framework for assessing transcriptional changes and characterizing heterogeneity in single-cell RNA sequencing data. Genome Biol 16, 278. 10.1186/s13059-015-0844-5. [PubMed: 26653891]

157. Trapnell C, Cacchiarelli D, Grimsby J, Pokharel P, Li S, Morse M, Lennon NJ, Livak KJ, Mikkelsen TS, and Rinn JL (2014). The dynamics and regulators of cell fate decisions are revealed by pseudotemporal ordering of single cells. Nat Biotechnol 32, 381–386. 10.1038/nbt.2859. [PubMed: 24658644]

Author Manuscript

Author Manuscript

Author Manuscript

Highlights:

$CD103^+CD4^+$ T_{RM} cell frequencies are increased in a subset of severe asthmatics

$CD103^+CD4^+$ T_{RM} cells in airways display T_H1, cytotoxic, and pro-inflammatory features

The $CD103^+CD4^+$ T_{RM}^{HIGH} endotype is associated with male late-onset severe asthma phenotype

Context and Significance:

Severe asthma is a heterogeneous chronic disease, characterized by persistent airway inflammation and remodeling refractory to current treatments. The current paradigm suggests that $CD4^+$ T_H2 cells play a central role in asthma pathogenesis. Although therapies targeting type 2 cytokines have shown promise, less than 50% of patients respond to treatments, and effects are neither durable nor reverse airway remodeling, which progressively lead to permanent airflow obstruction. Researchers from the La Jolla Institute for Immunology and the University of Southampton profiled the single-cell transcriptomes of airway T cells from severe asthmatics and discovered the presence of airway tissue-resident cytotoxic CD4 T cells that may play an important role in asthma pathogenesis. This important discovery opens a new avenue for a better stratification of severe asthma patients and new therapies.

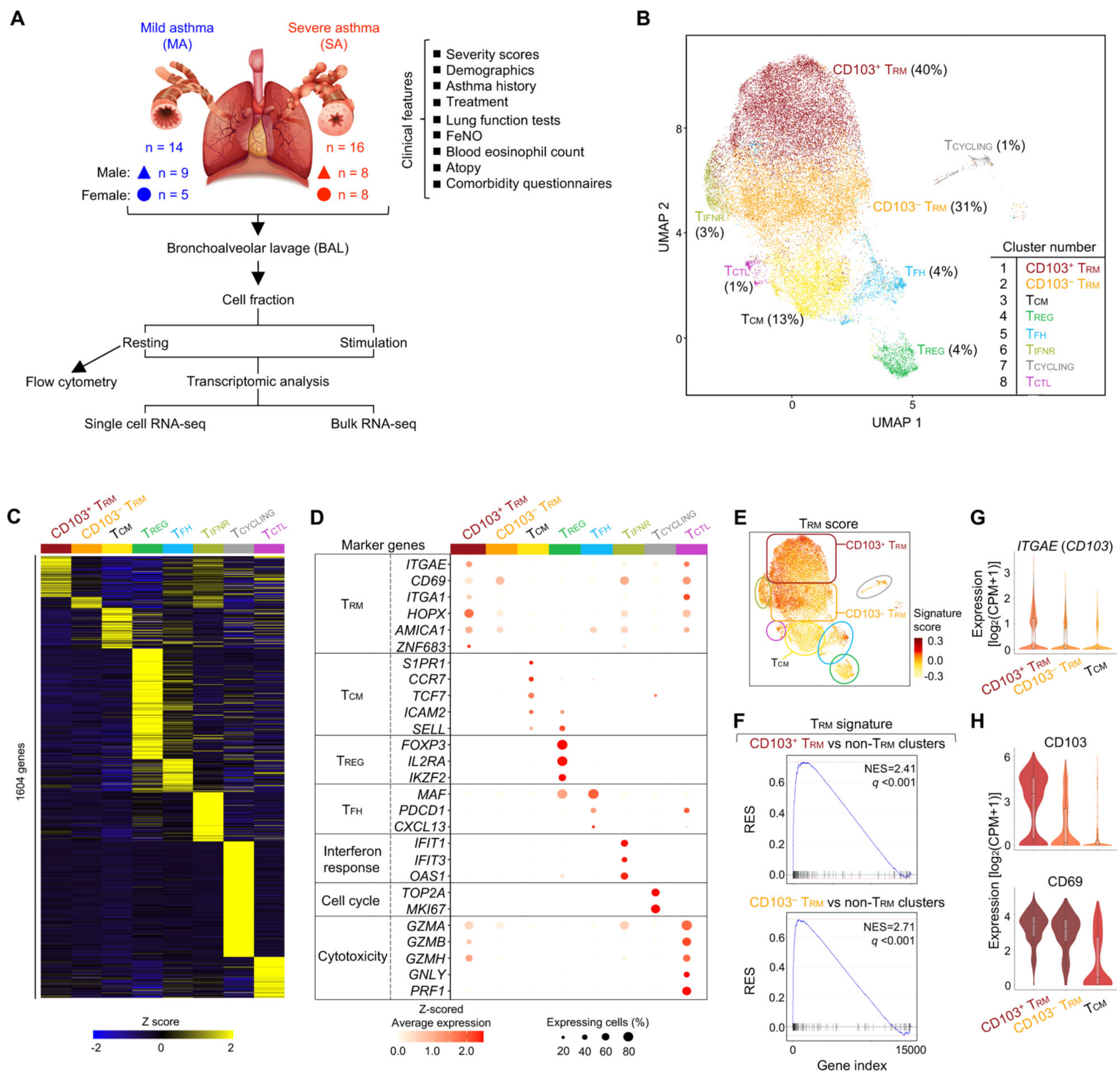

Figure 1. Single-cell transcriptomic analysis reveals heterogeneity among airway CD4$^+$ T cells.
(A) Study overview. **(B)** Uniform manifold approximation and projection (UMAP) visualization of Seurat-based clustering analysis of 27,771 single-cell transcriptomes of *ex vivo* sorted CD4$^+$ T cells obtained from 9 mild and 16 severe asthmatic patients. Each dot represents a cell and is colored based on cluster type. Proportion of cells in each cluster is shown (parenthesis). **(C)** Heatmap of row-wise z-score-normalized mean expression of significantly enriched transcripts in each cluster. Adjusted *P*-value < 0.05 and $\log_2$ (fold change) > 0.25. **(D)** Row-wise z-score-normalized mean expression (color scale) and percent of expressing cells (size scale) plot for a selection of marker genes in each cluster. **(E)** UMAP shows T_{RM} signature score (color scale) for each cell. Clusters are delineated by colored lines. **(F)** GSEA between CD103$^+$ T_{RM} cluster (top) and CD103$^-$ T_{RM} cluster (bottom) *versus* all non-T_{RM} clusters using published T_{RM} signature gene lists (Table

S3A). NES, normalized enrichment score; q, false discovery rate. **(G)** Violin plot displays normalized expression of *ITGAE* (*CD103*) in T_{RM} clusters ($CD103^+$ T_{RM} and $CD103^–$ T_{RM}) compared to T_{CM} cluster. **(H)** Violin plots show normalized protein expression of CD103 and CD69 in T_{RM} clusters compared to T_{CM} cluster (analysis done for 6 severe asthmatic patients).

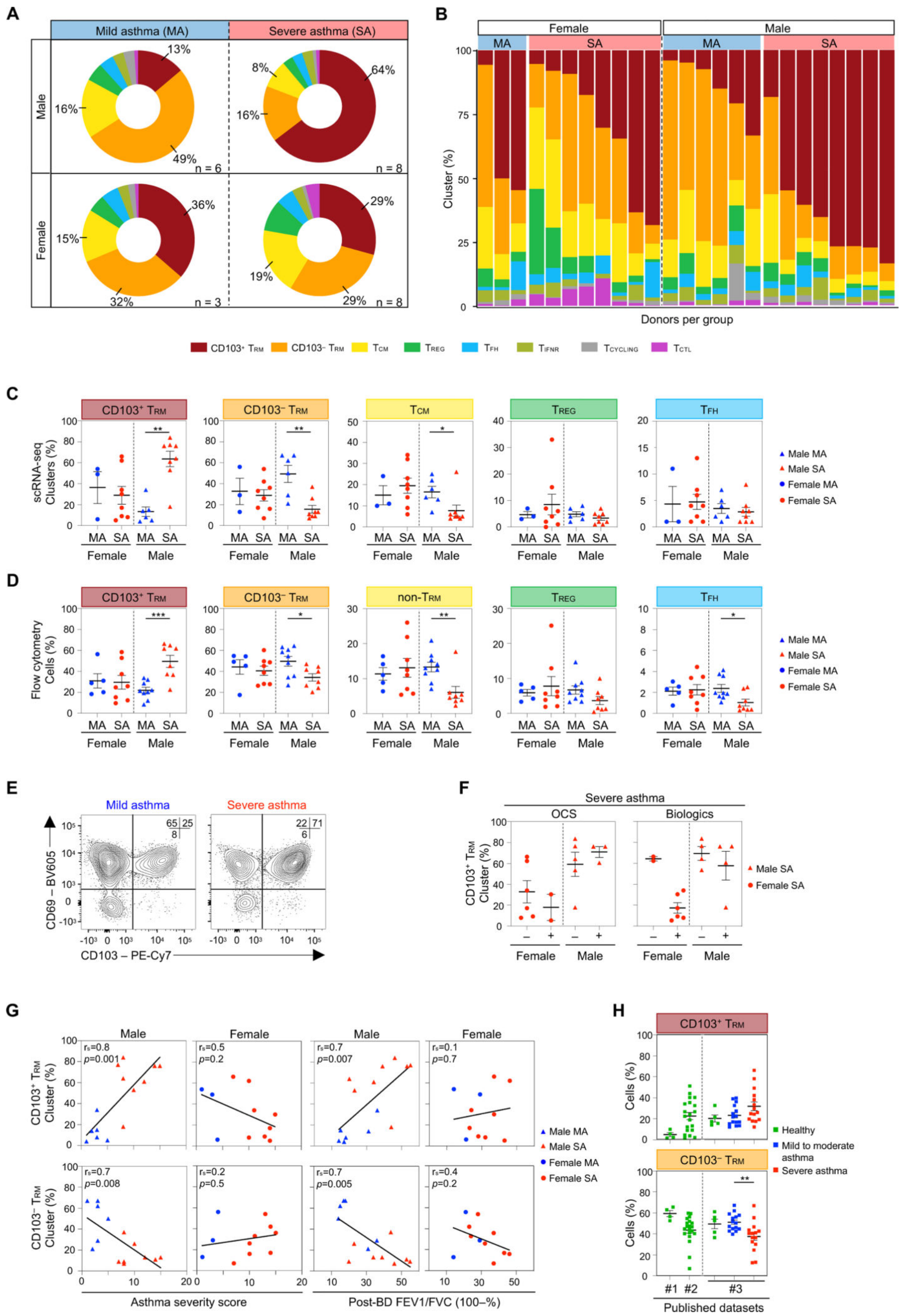

Figure 2. CD103$^+$ T$_{RM}$ cells are significantly increased in the airways of males with severe asthma.

(A) Pie charts represent average proportions of CD4$^+$ T cell subsets in the 4 clinical groups: mild asthmatic (MA) and severe asthmatic (SA) patients separated by sex. Colors correspond to cluster type. **(B)** Normalized stacked bar charts represent the proportions of CD4$^+$ T cell clusters per donor for the 4 clinical groups. Colors correspond to cluster type. **(C)** Dot plots show proportions of CD103$^+$ T$_{RM}$, CD103$^-$ T$_{RM}$, T$_{CM}$, T$_{REG}$, and T$_{FH}$ clusters for the 4 clinical groups (*, P < 0.05; **, P < 0.01; Mann-Whitney U test). **(D)** Dot plots show proportions of CD103$^+$ T$_{RM}$, CD103$^-$ T$_{RM}$, non-T$_{RM}$, T$_{REG}$, and T$_{FH}$ cells for the 4 clinical groups (*, $P < 0.05$; **, $P < 0.01$; ***, $P < 0.001$; Mann-Whitney U test). **(E)** Representative contour plot showing the expression of CD69 *versus* CD103 from CD4$^+$ T cells by flow cytometry from two donors, one mild and one severe asthmatic. **(F)** Dot plots show proportions of CD103$^+$ T$_{RM}$ cluster in severe asthmatics off (–) or on (+) oral corticosteroids (OCS; left) or biologics (right) treatment separated by sex (Mann-Whitney U test). **(G)** Scatter correlation plots between proportions of cells in CD103$^+$ T$_{RM}$ (top) or CD103$^-$ T$_{RM}$ (bottom) cluster with clinical features (composite asthma severity score and 100% - post-bronchodilator FEV1/FVC %). Each dot represents data from a single patient and are colored and shaped based on the 4 clinical groups. Correlation coefficient r and P value were computed using Spearman correlation analysis (trendline black). (**H**) Dot plots show proportions of CD4$^+$CD69$^+$CD103$^+$ T$_{RM}$ cells (top) and CD4$^+$CD69$^+$CD103$^-$ T$_{RM}$ cells (bottom) in BAL samples measured by flow cytometry from healthy (green) donors and asthmatic (blue = mild to moderate asthma; red = severe asthma) donors (unspecified sex) (**, $P < 0.01$; Kruskal-Wallis one-way test followed by Dunn's post-hoc test). Data obtained from published datasets #1,[44] #2,[45] and #3.[29] **(C, D, F, H)** Each dot represents data from a single subject, bars represent the mean, and t-lines represent SEM.

Author Manuscript
Author Manuscript
Author Manuscript

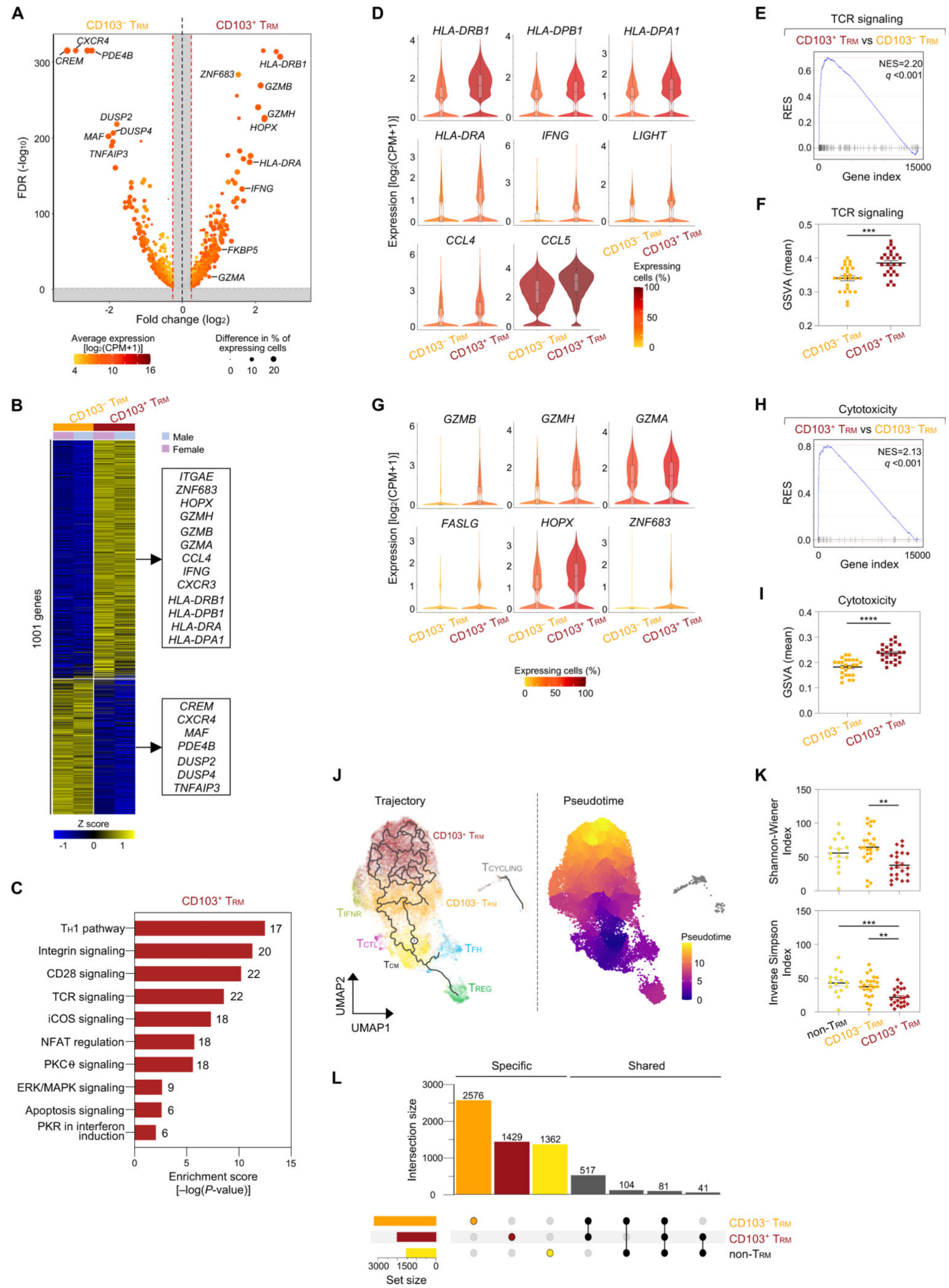

Figure 3. CD103⁺ T_{RM} subset displays qualitative features linked to TCR activation and cytotoxicity.

(A) Volcano plot shows false discovery rate (FDR) (-$\log_{10}$ adjusted *P*-value) and $\log_2$ (fold change) in expression for genes differentially expressed in CD103⁺ T_{RM} *versus* CD103⁻ T_{RM} clusters using sex as covariate. Dots are colored according to the mean of expression ($\log_2$) and sized based on the difference in the percentage of cells expressing the given gene, both derived from the group in which the gene is upregulated. Gray dotted lines represent the statistical threshold values: $\log_2$(fold change) > 0.25 and -$\log_{10}$(FDR > 1.3 (adjusted

P-value < 0.05). **(B)** Heatmap of row-wise z-score-normalized mean expression of 1001 differentially expressed genes between CD103$^+$ T$_{RM}$ and CD103$^-$ T$_{RM}$ clusters in male and female patients separately. Adjusted *P*-value < 0.05 and log$_2$ (fold change) > 0.25. **(C)** IPA shows top 10 pathways enriched for genes with increased expression in CD103$^+$ T$_{RM}$ cluster compared to CD103$^-$ T$_{RM}$ cluster. Numbers show matching genes from dataset and IPA gene lists (Table S3B). **(D, G)** Violin plots show normalized expression for example genes up-regulated in CD103$^+$ T$_{RM}$ cluster linked to TCR signaling **(D)** or cytotoxicity **(G)**. Color code represents the fraction of cells expressing the indicated gene in each cluster. **(E, H)** GSEA shows enrichment of genes linked to TCR signaling **(E)** or cytotoxicity **(H)** in CD103$^+$ T$_{RM}$ cluster compared to CD103$^-$ T$_{RM}$ cluster. NES, normalized enrichment score; q, false discovery rate. **(F, I)** GSVA shows TCR signaling **(F)** or cytotoxicity **(I)** enrichment scores per donor in CD103$^+$ T$_{RM}$ and CD103$^-$ T$_{RM}$ clusters (***, P < 0.001 and ****, P < 0.0001, respectively; Mann-Whitney U test). **(E, F, H, I)** Gene lists in Table S3A. **(J)** Single-cell pseudotime trajectory analysis of airway CD4$^+$ T cell subsets. Trajectory constructed using the Monocle3 algorithm. **(K)** Dot plots show Shannon-Wiener (top) and Inverse Simpson (bottom) TCR diversity indexes in bulk samples from CD103$^+$ T$_{RM}$, CD103$^-$ T$_{RM}$, and non-T$_{RM}$ cells (**, P < 0.01; ***, P < 0.001; Kruskal-Wallis one-way test followed by Dunn's post-hoc test). **(F, I, K)** Each dot represents data from a single patient, bars represent the mean, and t-lines represent SEM. **(L)** Bar chart shows number of TCR clonotypes specific (left) or shared (right) between bulk samples from CD103$^+$ T$_{RM}$, CD103$^-$ T$_{RM}$, and non-T$_{RM}$ cells. Total number of clones in each sample group (left bottom corner) is shown.

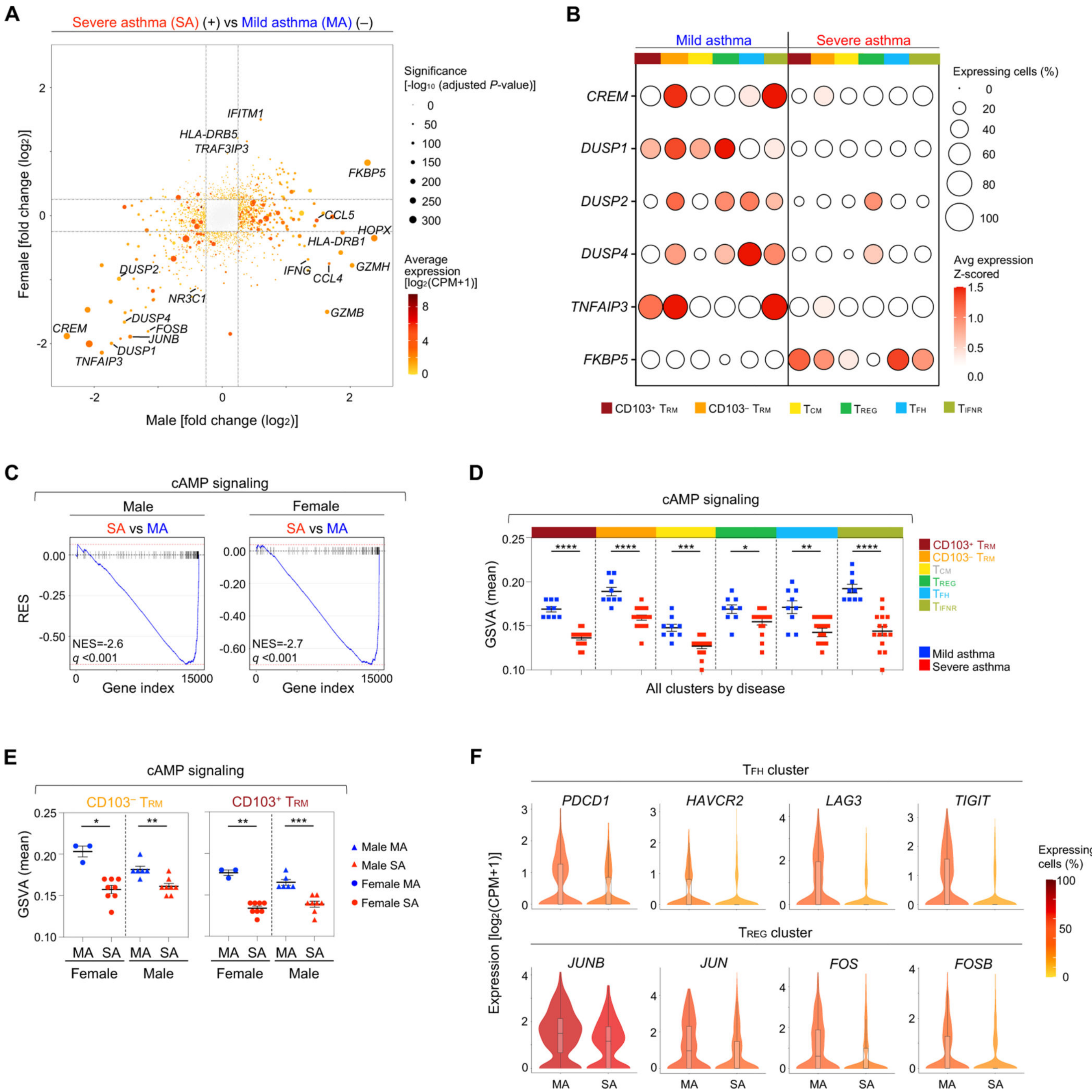

Figure 4. Molecules that restrain T cell activation and effector functions are reduced in severe asthma.

(A) Crater plot shows the $\log_2$ (fold change) expression of genes between severe and mild asthma in males (x-axis) and females (y-axis). Dotted lines indicate the statistical threshold value of fold change for gene filtering (adjusted *P*-value < 0.05 and $\log_2$ (fold change) > 0.25). **(B)** Plot shows row-wise z-score-normalized mean expression (color scale) and percent of expressing cells (size scale) for indicated genes in each cluster per disease. **(C)** GSEA plot shows enrichment of genes linked to cAMP immunoregulation pathway in cells from severe compared to mild asthmatics, in males (left) and females (right). NES, normalized enrichment score; q, false discovery rate. **(D, E)** GSVA shows cAMP signaling enrichment scores per donor grouped by disease per cluster **(D)** or per donor in CD103$^-$ T_{RM} (left) and CD103$^+$ T_{RM} (right) clusters for the 4 clinical groups **(E)** (*, $P < 0.05$; **, $P < 0.01$; ***, $P < 0.001$; ****, $P < 0.0001$; Mann-Whitney U test). **(C, D, E)** Gene lists in Table S3A. **(F)** Violin plots show normalized expression for genes down-regulated in severe asthma in the T_{FH} (top) and T_{REG} (bottom) clusters. Color code represents the fraction of cells expressing the indicated gene in each cluster.

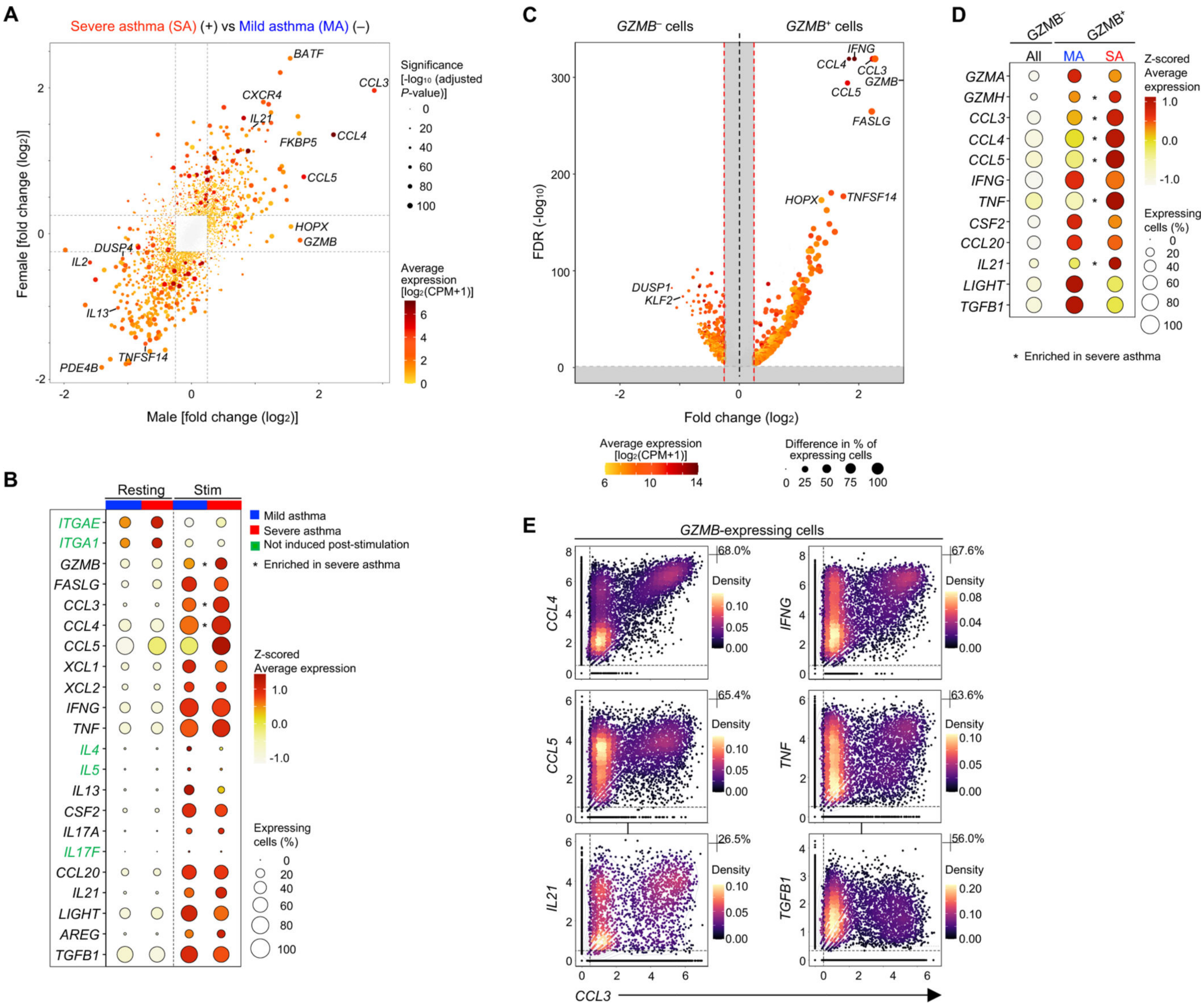

Figure 5. Pro-inflammatory cytokines are expressed by airway CD4$^+$ T cells from severe asthmatics.

(A) Crater plot shows the $\log_2$ (fold change) expression of genes between severe and mild asthma in males (x-axis) and females (y-axis). Dotted lines indicate the statistical threshold value of fold change for gene filtering (adjusted *P*-value < 0.05 and $\log_2$ (fold change) > 0.25). **(B)** Plot shows row-wise z-score-normalized mean expression (color scale) and percent of expressing cells (size scale) for indicated genes in resting and stimulation conditions per disease. **(C)** Volcano plot shows false discovery rate (FDR) ($-\log_{10}$ adjusted *P*-value) and $\log_2$ (fold change) in expression for genes differentially expressed in *GZMB*$^+$ cells *versus GZMB*$^-$ cells. Dots are colored according to the mean of expression ($\log_2$) and sized based on the difference in the percentage of cells expressing the given gene, both derived from the group in which the gene is up-regulated. Gray dotted lines represent the statistical threshold values: $\log_2$(fold change) > 0.25 and $-\log_{10}$(FDR > 1.3 (adjusted *P*-value < 0.05). **(D)** Plot shows row-wise z-score-normalized mean expression (color scale) and percent of expressing cells (size scale) for indicated genes in all *GZMB*$^-$, mild asthma

(MA) *GZMB*$^+$, and severe asthma (SA) *GZMB*$^+$ cells. **(E)** Scatter plots show co-expression of *CCL3* with other cytokine genes transcripts in *GZMB*-expressing CD4$^+$ T cells in stimulation condition. Percentage of co-expressing cells is indicated (top right). Each dot represents one cell. Cells are colored based on density value. Dotted lines indicate threshold of Seurat normalized gene expression (log2FC) (> 0.5).

Key resources table

REAGENT or RESOURCE	SOURCE	IDENTIFIER
Antibodies		
Anti-Human CD45 (2D1) - Alexa Fluor 700	BioLegend	Cat# 368514; RRID: AB_2566374
Anti-Human CD3 (SK7) - APC-Cy7	BioLegend	Cat# 344818; RRID: AB_10645474
Anti-Human CD8a (RPA-T8) - BV570	BioLegend	Cat# 301038; RRID: AB_2563213
Anti-Human CD4 (RPA-T4) – BV510	BioLegend	Cat# 300546; RRID: AB_2563314
Anti-Human CD357/GITR (108–17) – BV711	BioLegend	Cat# 371212; RRID: AB_2687161
Anti-Human CD185/CXCR5 (RF8B2) – BV421	BD Biosciences	Cat# 562747; RRID: AB_2737766
Anti-Human CD25 (2A3) – BB515	BD Biosciences	Cat# 564467; RRID: AB_2744340
Anti-Human CD127 (eBioRDR5) - APC	eBioscience	Cat# 17–1278-42; RRID: AB_1659670
Anti-Human CD69 (FN50) – BV605	BioLegend	Cat# 310938; RRID: AB_2562307
Anti-Human CD103 (Ber-ACT8) – PE-Cy7	BioLegend	Cat# 350212; RRID: AB_2561599
Anti-Human FcR Blocking Reagent	Miltenyi Biotec	Cat# 130–059-901
Anti-Human CD103 (Ber-ACT8) - TotalSeq-A	BioLegend	Cat# 350231; RRID: AB_2749996
Anti-Human CD69 (FN50) - TotalSeq-A	BioLegend	Cat# 310947; RRID: AB_2749997
Biological samples		
Human bronchoalveolar lavage (BAL) samples	This paper	Protocol number IRB VD-156–1118
Chemicals, peptides, and recombinant proteins		
Recombinant RNAse inhibitor	Takara Bio	Cat# 2313B
PMA (Phorbol 12-myristate 13-acetate)	Sigma-Aldrich	Cat# P8139–1MG
Ionomycin (calcium salt)	Sigma-Aldrich	Cat# I0634–1MG
Brilliant Stain Buffer Plus	BD Biosciences	Cat# 566385
Propidium Iodide solution	Sigma-Aldrich	Cat# P4864
Critical commercial assays		
Chromium Single Cell 3’GEM Kit v3	10x Genomics	Cat# PN-1000077
Chromium Single Cell 3′ Library Kit v3	10x Genomics	Cat# PN-1000078
Chromium Single Cell 3′ Gel Bead Kit v3	10x Genomics	Cat# PN-1000076
Chromium Chip B Single Cell Kit	10x Genomics	Cat# PN-1000073
Chromium i7 Multiplex Kit	10x Genomics	Cat# PN-120262
Chromium Single Cell 3′ Feature Barcode Library Kit	10x Genomics	Cat# PN-1000079
Nextera XT DNA Library Preparation Kit	Illumina	Cat# FC-131–1096

REAGENT or RESOURCE	SOURCE	IDENTIFIER
DNeasy Blood and Tissue Kit	Qiagen	Cat# 69506
Infinium Multi-Ethnic Global-8 v1.0 Kit	Illumina	Cat# WG-316–1001
Deposited data		
Bulk RNA-sequencing data	This paper	GEO: GSE181709
Single-cell RNA-sequencing data	This paper	GEO: GSE181710
Combined bulk and single-cell RNA-sequencing data contained in GSE181709 and GSE181710	This paper	GEO: GSE181711
Original code	Zenodo https://doi.org/10.5281/zenodo.8342757	N/A
Software and algorithms		
FlowJo v10.7.1	FlowJo	https://www.flowjo.com/
Prism 9	Graphpad	https://www.graphpad.com
IPA (Ingenuity Pathway Analysis)	Qiagen	www.qiagen.com/ingenuity
Cell Ranger v3.1.0	10x Genomics	https://www.10xgenomics.com
Seurat v3.0.2	(Stuart et al., 2019)	https://www.satijalab.org/seurat
R v4.0.1	R Core team	www.R-project.org
DESeq2 v1.16.1	(Love et al., 2014)	http://www.bioconductor.org/packages/release/bioc/html/DESeq2.html
ComplexUpset v1.3.3	(Lex et al., 2014)	https://github.com/krassowski/complex-upset
Monocle3 v1.0.0	(Trapnell et al., 2014)	https://github.com/cole-trapnell-lab/monocle3
MAST v1.8.2	(Finak et al., 2015)	https://github.com/RGLab/MAST
MiXCR v2.1.10	(Bolotin et al., 2015)	http://mixcr.milaboratory.com/
vdjtools software v1.2.1	(Shugay et al., 2015)	https://github.com/mikessh/vdjtools
FGSEA v1.10.1	(Korotkevich et al., 2021)	https://bioconductor.org/packages/release/bioc/html/fgsea.html
clusterProfiler v4.6.2	(Wu et al., 2021)	https://github.com/GuangchuangYu/enrichment4GTEx_clusterProfiler
SCGSVA v0.0.14	(Hänzelmann et al., 2013)	https://github.com/guokai8/scGSVA
Other		
Smart-seq2 protocol	(Picelli et al., 2013) (Rosales et al., 2018)	https://www.nature.com/articles/nmeth.2639 https://link.springer.com/protocol/10.1007/978–1-4939–7896-0_21